FOUNDATIONS IN GLAUCOMA

Proceedings of the 4th Annual Educators Meeting of the Optometric Glaucoma Foundation

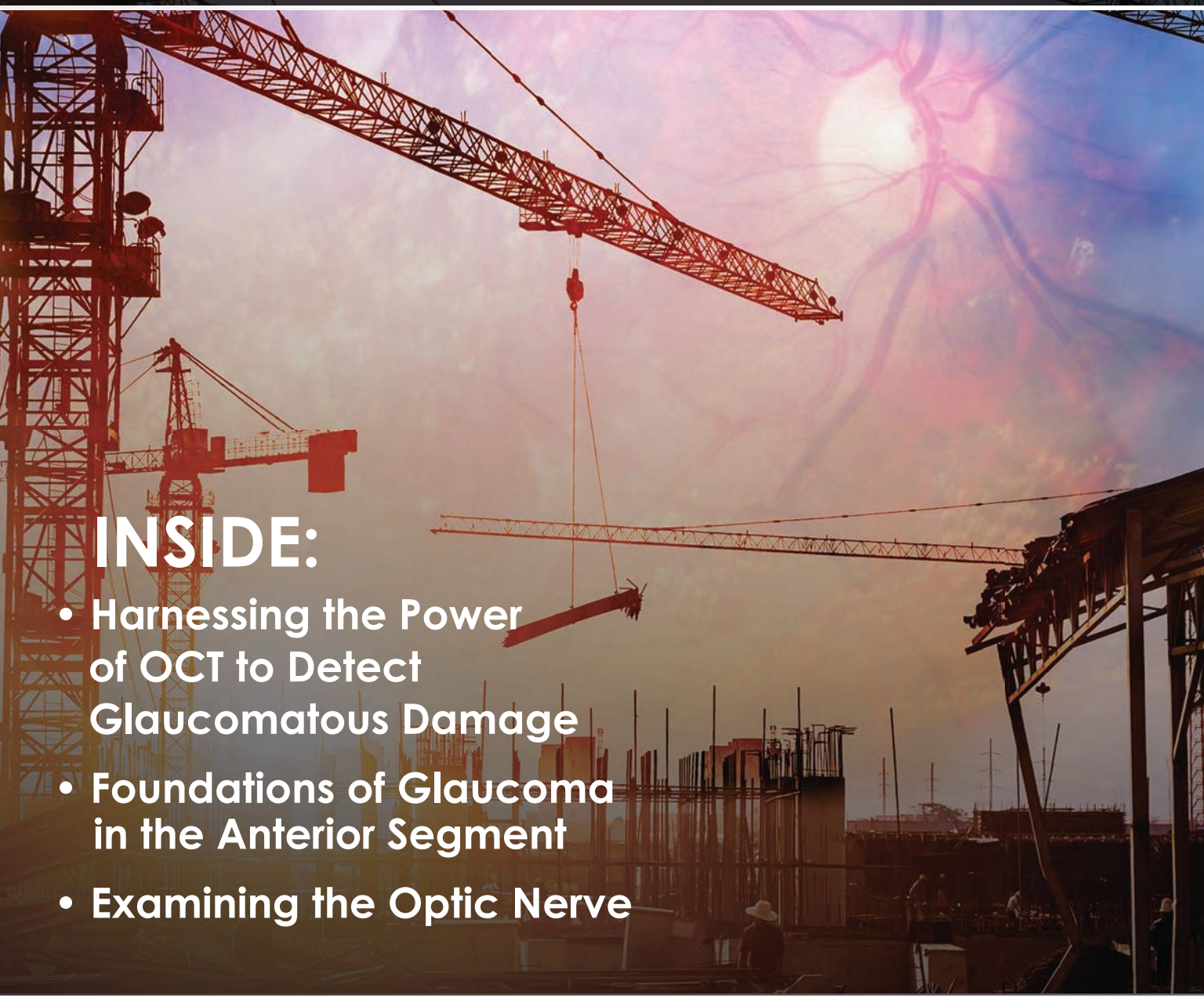

INSIDE:

- Harnessing the Power of OCT to Detect Glaucomatous Damage
- Foundations of Glaucoma in the Anterior Segment
- Examining the Optic Nerve

Sponsored by

BAUSCH + LOMB

Supplement to

REVIEW of OPTOMETRY

March 2021

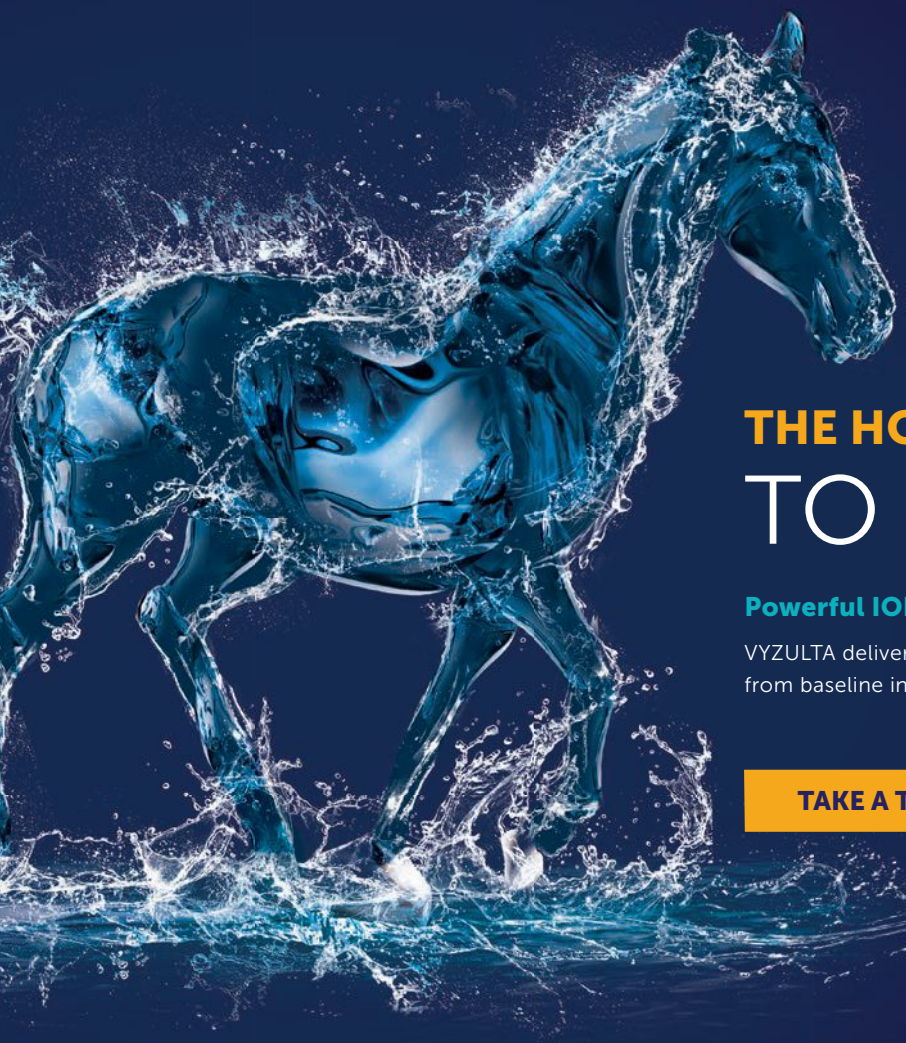

VYZULTA®
(latanoprostene bunod ophthalmic solution), 0.024%

THE HORSEPOWER YOU NEED TO LOWER IOP

Powerful IOP reduction with excellent tolerability[1,2]

VYZULTA delivered **up to 9.1 mmHg mean IOP reduction** from baseline in pivotal trials.[1,2*]

TAKE A TEST RIDE AT VYZULTAHCP.COM

*Pivotal study designs: Two Phase 3, randomized, multicenter, parallel-group studies, APOLLO and LUNAR, evaluating noninferiority of once-daily VYZULTA vs twice-daily timolol maleate 0.5% in patients with open-angle glaucoma or ocular hypertension. Primary endpoint was IOP measured at 9 assessment time points in study eye. APOLLO (VYZULTA, n=284; timolol, n=133) and LUNAR (VYZULTA, n=278; timolol, n=136).[2,3]

INDICATION

VYZULTA® (latanoprostene bunod ophthalmic solution), 0.024% is indicated for the reduction of intraocular pressure (IOP) in patients with open-angle glaucoma or ocular hypertension.

IMPORTANT SAFETY INFORMATION

- Increased pigmentation of the iris and periorbital tissue (eyelid) can occur. Iris pigmentation is likely to be permanent
- Gradual changes to eyelashes, including increased length, increased thickness, and number of eyelashes, may occur. These changes are usually reversible upon treatment discontinuation
- Use with caution in patients with a history of intraocular inflammation (iritis/uveitis). VYZULTA should generally not be used in patients with active intraocular inflammation
- Macular edema, including cystoid macular edema, has been reported during treatment with prostaglandin analogs. Use with caution in aphakic patients, in pseudophakic patients with a torn posterior lens capsule, or in patients with known risk factors for macular edema
- There have been reports of bacterial keratitis associated with the use of multiple-dose containers of topical ophthalmic products that were inadvertently contaminated by patients
- Contact lenses should be removed prior to the administration of VYZULTA and may be reinserted 15 minutes after administration
- Most common ocular adverse reactions with incidence ≥2% are conjunctival hyperemia (6%), eye irritation (4%), eye pain (3%), and instillation site pain (2%)

For more information, please see Brief Summary of full Prescribing Information on adjacent page.

References: 1. VYZULTA Prescribing Information. Bausch & Lomb Incorporated. **2.** Weinreb RN, Scassellati Sforzolini B, Vittitow J, Liebmann J. Latanoprostene bunod 0.024% versus timolol maleate 0.5% in subjects with open-angle glaucoma or ocular hypertension: the APOLLO study. *Ophthalmology.* 2016;123(5):965-973. **3.** Medeiros FA, Martin KR, Peace J, Scassellati Sforzolini B, Vittitow JL, Weinreb RN. Comparison of latanoprostene bunod 0.024% and timolol maleate 0.5% in open-angle glaucoma or ocular hypertension: the LUNAR study. *Am J Ophthalmol.* 2016;168:250-259.

BAUSCH + LOMB

BRIEF SUMMARY OF PRESCRIBING INFORMATION

This Brief Summary does not include all the information needed to use VYZULTA safely and effectively. See full Prescribing Information for VYZULTA.

VYZULTA® (latanoprostene bunod ophthalmic solution), 0.024%, for topical ophthalmic use.

Initial U.S. Approval: 2017

1 INDICATIONS AND USAGE

VYZULTA® (latanoprostene bunod ophthalmic solution) 0.024% is indicated for the reduction of intraocular pressure (IOP) in patients with open-angle glaucoma or ocular hypertension.

4 CONTRAINDICATIONS

None

5 WARNINGS AND PRECAUTIONS

5.1 Pigmentation

VYZULTA® (latanoprostene bunod ophthalmic solution), 0.024% may cause changes to pigmented tissues. The most frequently reported changes with prostaglandin analogs have been increased pigmentation of the iris and periorbital tissue (eyelid).

Pigmentation is expected to increase as long as latanoprostene bunod ophthalmic solution is administered. The pigmentation change is due to increased melanin content in the melanocytes rather than to an increase in the number of melanocytes. After discontinuation of VYZULTA, pigmentation of the iris is likely to be permanent, while pigmentation of the periorbital tissue and eyelash changes are likely to be reversible in most patients. Patients who receive prostaglandin analogs, including VYZULTA, should be informed of the possibility of increased pigmentation, including permanent changes. The long-term effects of increased pigmentation are not known.

Iris color change may not be noticeable for several months to years. Typically, the brown pigmentation around the pupil spreads concentrically towards the periphery of the iris and the entire iris or parts of the iris become more brownish. Neither nevi nor freckles of the iris appear to be affected by treatment. While treatment with VYZULTA® (latanoprostene bunod ophthalmic solution), 0.024% can be continued in patients who develop noticeably increased iris pigmentation, these patients should be examined regularly *[see Patient Counseling Information (17) in full Prescribing Information]*.

5.2 Eyelash Changes

VYZULTA may gradually change eyelashes and vellus hair in the treated eye. These changes include increased length, thickness, and the number of lashes or hairs. Eyelash changes are usually reversible upon discontinuation of treatment.

5.3 Intraocular Inflammation

VYZULTA should be used with caution in patients with a history of intraocular inflammation (iritis/uveitis) and should generally not be used in patients with active intraocular inflammation as it may exacerbate this condition.

5.4 Macular Edema

Macular edema, including cystoid macular edema, has been reported during treatment with prostaglandin analogs. VYZULTA should be used with caution in aphakic patients, in pseudophakic patients with a torn posterior lens capsule, or in patients with known risk factors for macular edema.

5.5 Bacterial Keratitis

There have been reports of bacterial keratitis associated with the use of multiple-dose containers of topical ophthalmic products. These containers had been inadvertently contaminated by patients who, in most cases, had a concurrent corneal disease or a disruption of the ocular epithelial surface.

5.6 Use with Contact Lens

Contact lenses should be removed prior to the administration of VYZULTA because this product contains benzalkonium chloride. Lenses may be reinserted 15 minutes after administration.

6 ADVERSE REACTIONS

The following adverse reactions are described in the Warnings and Precautions section: pigmentation (5.1), eyelash changes (5.2), intraocular inflammation (5.3), macular edema (5.4), bacterial keratitis (5.5), use with contact lens (5.6).

6.1 Clinical Trials Experience

Because clinical trials are conducted under widely varying conditions, adverse reaction rates observed in the clinical trials of a drug cannot be directly compared to rates in the clinical trials of another drug and may not reflect the rates observed in practice.

VYZULTA was evaluated in 811 patients in 2 controlled clinical trials of up to 12 months duration. The most common ocular adverse reactions observed in patients treated with latanoprostene bunod were: conjunctival hyperemia (6%), eye irritation (4%), eye pain (3%), and instillation site pain (2%). Approximately 0.6% of patients discontinued therapy due to ocular adverse reactions including ocular hyperemia, conjunctival irritation, eye irritation, eye pain, conjunctival edema, vision blurred, punctate keratitis and foreign body sensation.

8 USE IN SPECIFIC POPULATIONS

8.1 Pregnancy

Risk Summary

There are no available human data for the use of VYZULTA during pregnancy to inform any drug associated risks.

Latanoprostene bunod has caused miscarriages, abortion, and fetal harm in rabbits. Latanoprostene bunod was shown to be abortifacient and teratogenic when administered intravenously (IV) to pregnant rabbits at exposures ≥ 0.28 times the clinical dose. Doses ≥ 20 µg/kg/day (23 times the clinical dose) produced 100% embryofetal lethality. Structural abnormalities observed in rabbit fetuses included anomalies of the great vessels and aortic arch vessels, domed head, sternebral and vertebral skeletal anomalies, limb hyperextension and malrotation, abdominal distension and edema. Latanoprostene bunod was not teratogenic in the rat when administered IV at 150 mcg/kg/day (87 times the clinical dose) *[see Data]*.

The background risk of major birth defects and miscarriage for the indicated population is unknown. However, the background risk in the U.S. general population of major birth defects is 2 to 4%, and of miscarriage is 15 to 20%, of clinically recognized pregnancies.

Data

Animal Data

Embryofetal studies were conducted in pregnant rabbits administered latanoprostene bunod daily by intravenous injection on gestation days 7 through 19, to target the period of organogenesis. The doses administered ranged from 0.24 to 80 mcg/kg/day. Abortion occurred at doses ≥ 0.24 mcg/kg/day latanoprostene bunod (0.28 times the clinical dose, on a body surface area basis, assuming 100% absorption). Embryofetal lethality (resorption) was increased in latanoprostene bunod treatment groups, as evidenced by increases in early resorptions at doses ≥ 0.24 mcg/kg/day and late resorptions at doses ≥ 6 mcg/kg/day (approximately 7 times the clinical dose). No fetuses survived in any rabbit pregnancy at doses of 20 mcg/kg/day (23 times the clinical dose) or greater. Latanoprostene bunod produced structural abnormalities at doses ≥ 0.24 mcg/kg/day (0.28 times the clinical dose). Malformations included anomalies of sternum, coarctation of the aorta with pulmonary trunk dilation, retroesophageal subclavian artery with absent brachiocephalic artery, domed head, forepaw hyperextension and hindlimb malrotation, abdominal distention/edema, and missing/fused caudal vertebrae.

An embryofetal study was conducted in pregnant rats administered latanoprostene bunod daily by intravenous injection on gestation days 7 through 17, to target the period of organogenesis. The doses administered ranged from 150 to 1500 mcg/kg/day. Maternal toxicity was produced at 1500 mcg/kg/day (870 times the clinical dose, on a body surface area basis, assuming 100% absorption), as evidenced by reduced maternal weight gain. Embryofetal lethality (resorption and fetal death) and structural anomalies were produced at doses ≥ 300 mcg/kg/day (174 times the clinical dose). Malformations included anomalies of the sternum, domed head, forepaw hyperextension and hindlimb malrotation, vertebral anomalies and delayed ossification of distal limb bones. A no observed adverse effect level (NOAEL) was established at 150 mcg/kg/day (87 times the clinical dose) in this study.

8.2 Lactation

Risk Summary

There are no data on the presence of VYZULTA in human milk, the effects on the breastfed infant, or the effects on milk production. The developmental and health benefits of breastfeeding should be considered, along with the mother's clinical need for VYZULTA, and any potential adverse effects on the breastfed infant from VYZULTA.

8.4 Pediatric Use

Use in pediatric patients aged 16 years and younger is not recommended because of potential safety concerns related to increased pigmentation following long-term chronic use.

8.5 Geriatric Use

No overall clinical differences in safety or effectiveness have been observed between elderly and other adult patients.

13 NONCLINICAL TOXICOLOGY

13.1 Carcinogenesis, Mutagenesis, Impairment of Fertility

Latanoprostene bunod was not mutagenic in bacteria and did not induce micronuclei formation in the *in vivo* rat bone marrow micronucleus assay. Chromosomal aberrations were observed *in vitro* with human lymphocytes in the absence of metabolic activation.

Latanoprostene bunod has not been tested for carcinogenic activity in long-term animal studies. Latanoprost acid is a main metabolite of latanoprostene bunod. Exposure of rats and mice to latanoprost acid, resulting from oral dosing with latanoprost in lifetime rodent bioassays, was not carcinogenic.

Fertility studies have not been conducted with latanoprostene bunod. The potential to impact fertility can be partially characterized by exposure to latanoprost acid, a common metabolite of both latanoprostene bunod and latanoprost. Latanoprost acid has not been found to have any effect on male or female fertility in animal studies.

13.2 Animal Toxicology and/or Pharmacology

A 9-month toxicology study administered topical ocular doses of latanoprostene bunod to one eye of cynomolgus monkeys: control (vehicle only), one drop of 0.024% bid, one drop of 0.04% bid and two drops of 0.04% per dose, bid. The systemic exposures are equivalent to 4.2-fold, 7.9-fold, and 13.5-fold the clinical dose, respectively, on a body surface area basis (assuming 100% absorption). Microscopic evaluation of the lungs after 9 months observed pleural/subpleural chronic fibrosis/inflammation in the 0.04% dose male groups, with increasing incidence and severity compared to controls. Lung toxicity was not observed at the 0.024% dose.

U.S. Patent Numbers: 7,273,946; 7,629,345; 7,910,767; 8,058,467.

VYZULTA is a trademark of Bausch & Lomb Incorporated or its affiliates.

Distributed by:

Bausch + Lomb, a division of

Bausch Health US, LLC

Bridgewater, NJ 08807 USA

Based on 9612403 (Folded), 9612303 (Flat) 5/2019

VYZ.0109.USA.20 Issued: 5/2020

TABLE OF CONTENTS

The 4th Annual Educators Meeting of the Optometric Glaucoma Foundation (OGF), held virtually on Sept. 12, 2020, brought together three recognized leaders in the field of glaucoma, who shared foundational insights on evaluating OCT scans for glaucomatous damage, understanding pathophysiology in the anterior segment leading to disease, and examining the optic nerve. The Educators meeting was developed as a resource for educators who teach glaucoma at the schools and colleges of optometry.

Donald C. Hood, PhD, the James F. Bender Professor of Psychology and professor of ophthalmic science at Columbia University, gave a comprehensive overview of optical coherence tomography (OCT) and offered expert wisdom for understanding OCT reports. He was frank about the fact that clinicians who care for glaucoma patients are increasingly relying on OCT, but many are not taking full advantage of this powerful technology. Dr. Hood laid out a roadmap for the best way to look at and evaluate OCT reports, and drove home a key message: Eye care professionals must move beyond relying on the reports' summary metrics to understand their patients' disease.

Next in the lineup was Thomas F. Freddo, OD, PhD, a Senior Fulbright Fellow and part-time professor of optometry at the MCP Health Sciences University in Worcester, Mass., who served for 25 years as professor of ophthalmology, pathology, and anatomy at Boston University School of Medicine, and then as professor and director of the School of Optometry and Vision Science at The University of Waterloo before retiring in 2016. Dr. Freddo, the recipient of the 2020 OGS Research Excellence Award, painted a multilayered picture of how dysregulation of natural processes in the anterior segment can create conditions leading to aqueous humor flow obstruction and elevated intraocular pressure.

He dove deeply into the characteristics of aqueous humor and mechanics of its production and flow, and revealed circumstances leading to dysfunction in the conventional and uveoscleral outflow pathways. He showed how some current and emerging therapies are designed to interrupt pathological processes and regulate outflow resistance in these pathways. Looking ahead, Dr. Freddo explained that nitric oxide donors, especially those that are butylated, are being targeted at the optic nerve head for potential therapeutic effect.

Rounding out the day, Peter Lalle, OD, FAAO, former chief of optometry at Baltimore VA Medical Center from 1981 to 2016, and a founding member of the Optometric Glaucoma Society, took on a universal problem he observed in many of his students and residents: They had difficulty evaluating the optic nerve. Dr. Lalle researched the issue to lay out a better way to teach optic nerve evaluation in today's digital world.

This supplement, developed by *Review of Optometry*, was made possible with generous support from Bausch + Lomb.

Please visit the OGS website (www.optometricglaucomasociety.org) to learn more about the society and how to apply for membership.

Murray Fingeret, OD
President, Optometric Glaucoma Foundation

OCT EVALUATION

Harnessing the Power of OCT to Detect Glaucomatous Damage

Donald C. Hood, PhD

While clinicians who care for glaucoma patients are increasingly relying on optical coherence tomography (OCT), many are not taking full advantage of this powerful technology.[1,2] First, clinicians often turn to summary metrics generated by OCT and visual field (VF) systems to make decisions about their patients' care.[1,2] But glaucoma is an optic neuropathy characterized by a specific pattern of anatomic and "behavioral" change, so we should be looking for patterns of damage observed across OCT and VF reports.[3,4] Second, OCT images of the retina have much better resolution than MRI scans, yet many clinician do not look at the images.

For clinicians to harness OCT's potential, they need to understand the relationship between the anatomical nature of glaucomatous damage and how it appears on OCT images and maps. This requires an understanding of some basic anatomy in addition to an awareness of the nature of glaucomatous damage as revealed by OCT, and knowledge about what to look for in reports produced by OCT devices.

ANATOMY REFRESHER

To better understand what OCT can teach us about the nature of glaucomatous damage, it is paramount to recall the anatomy of the retina, a small area of the brain situated in the posterior eye. As seen in Figure 1, light enters the eye and is absorbed in the outer retina, triggering electrochemical activity that is communicated when receptors synapse with bipolar and ganglion cells.

The cells reside in several layers. The outer nuclear layer houses the receptors, while the inner plexiform layer (IPL) contains the dendrites of ganglion cells, the retinal ganglion cell layer (RGCL), and the retinal nerve fiber layer (RNFL)—housing glial cells, blood vessels, and the axons of ganglion cells, which exit the retina as part of the optic nerve.

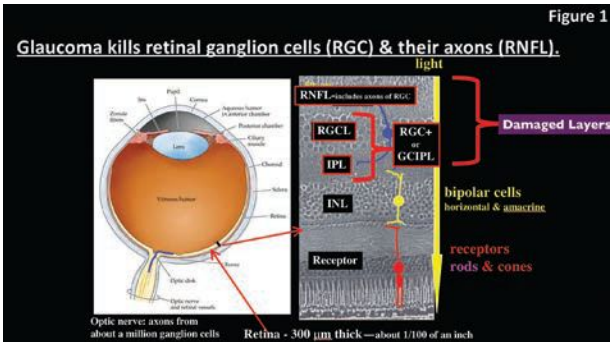

FIGURE 1. LAYERS DAMAGED IN GLAUCOMA
This figure illustrates the IPL, RGCL, and RNFL, which are damaged in glaucoma. *Images: Donald C. Hood, PhD*

Since glaucoma results in the death of RGCs and their axons, the layers damaged by disease are the IPL, RGCL, and RNFL; the combined RCGL plus IPL is referred to as the "retinal ganglion cell plus (+)", RGC+, or GCIPL.

Axons travel from the cell bodies of RGCs to the optic disc. During development, ganglion cell axons on the temporal side (away from the disc) arc around the bottom of the fovea and bunch in the inferior disc as shown in Figure 2. This region of the disc is particularly vulnerable to glaucomatous damage. The same is true for the area above the fovea, where the corresponding region of the upper (superior) disc is also at risk of damage. Due to the arcuate nature of the paths taken by the axons to the disc, and because glaucoma acts largely at, or in, the optic disc, glaucomatous damage has a characteristic arcuate shape as shown by the black regions in Figure 2. Because glaucoma exhibits this arcuate-shaped damage, clinicians should be looking for similar patterns of damage in the OCT reports and on VFs.

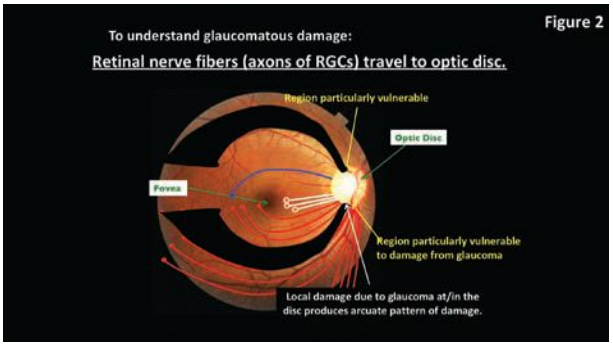

FIGURE 2. ARCUATE PATTERN OF DAMAGE
Due to biology and the nature of glaucoma, damage from the disease has a characteristic arcuate shape as it arcs away from the optic disc, above and below the fovea, as shown.

WHAT OCT SCANS REVEAL

OCT, a noninvasive measure of retinal anatomy, is similar to ultrasound but uses light instead of sound. Because light has a shorter wavelength, OCT has much higher resolution than ultrasound. Figure 3 shows the RGC+ and RNFL on a line scan through the fovea and a circular scan around the optic disc.

With early versions of the OCT, glaucoma specialists primarily had access to circumpapillary scans (i.e., "circle scans" around the disc). The resultant OCT images were displayed as flattened-out images, as shown in Figures 3 and 4D. More than 10 years ago, the Zeiss Stratus time-domain OCT was the only device available, and it was relatively slow, so its images were of poorer quality than those produced by today's instruments. The device generated a report that included an average circle scan

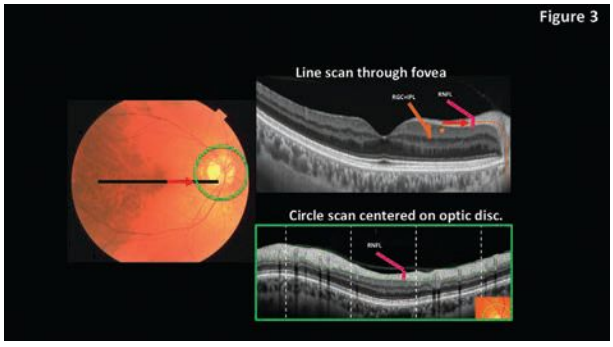

FIGURE 3. VISUALIZING LAYERS
The OCT circular scans here feature RGC+ and RNFL thickness information.

image based upon a scan that started in the temporal region and went to superior, nasal, inferior, and back to temporal (Figure 4D, bottom). As such, the resulting thickness plot (Figure 4C, red rectangle) was called a "TSNIT curve/plot." This report changed the way we approach glaucoma and was a major advance forward, even though the image was poor by today's standards.

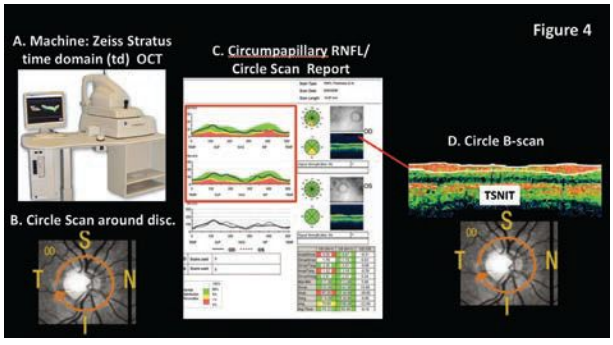

FIGURE 4. ZEISS STRATUS TIME DOMAIN
More than 10 years ago, the Zeiss Stratus time-domain OCT was the only OCT available, and it generated the glaucoma report shown in the middle column.

Over the last decade, newer OCT devices made by Zeiss and others began offering spectral-domain OCT. This method yields higher image resolution than time-domain OCT scans, and it affords a better view of the details of the RNFL, as seen in Figure 5 (upper panel).

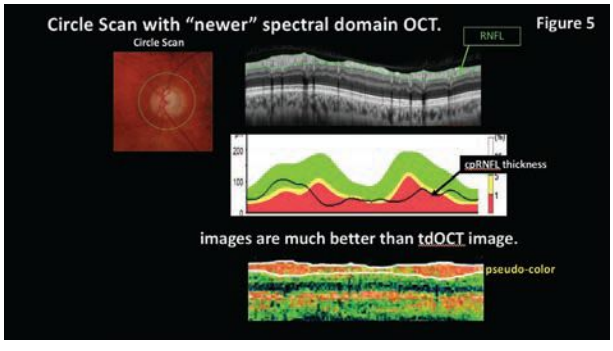

FIGURE 5. OCT IMPROVEMENTS
Over the last decade, OCT devices began offering spectral-domain, rather than time-domain, OCT, with higher resolution.

GETTING PERSPECTIVE ON OCT SCANS

By looking at a fundus photo, the clinician can often recognize RNF defects by locating an arcing darkened pattern starting at the optic disc, as seen on the photo in Figure 6A. An OCT circular scan image of this eye is shown in Figure 6B (middle panel; the inset in Figure 6A shows a portion of this image). To align the OCT images with the photo, the OCT image is shown as if it had been scanned from nasal around through temporal and back to nasal. The center of the NSTIN curve is now the temporal region of the retina. Flipping the NSTIN scan from horizontal to vertical and aligning it with the fundus photo shows the correspondence between regions of the photo and regions of the OCT circular image, as shown in Figure 6A. Notice that a segment of preserved RNFL and ganglion cells on the OCT scan corresponds to a normal-looking section of the fundus photo, to the left of the optic disc.

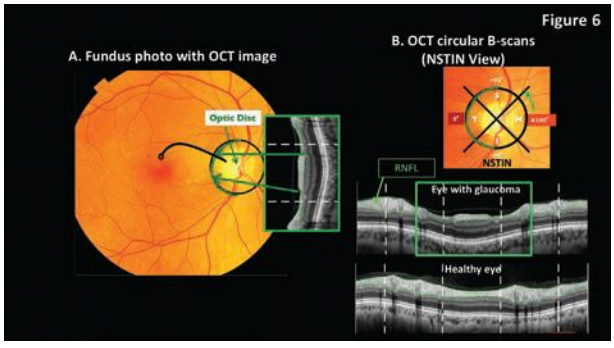

FIGURE 6. COMPARING OCT SCANS TO RETINAL PHOTOS
The OCT scan image is aligned in panel A to illustrate the relationship of damage seen on a fundus photo to RNFL thinning seen on OCT circular B-scans.

To better understand what is seen on OCT images, a few years ago we turned to adaptive optics scanning laser ophthalmoscopy (SLO).[5] Adaptive optics uses mirrors (instead of glass) as lenses to remove aberrations. We teamed with researchers Alfredo Dubra, PhD, associate professor of ophthalmology, Stanford University; Richard Rosen, MD, professor of ophthalmology, Mount Sinai School of Medicine; and Yuen Ping Toco Chiu, PhD, associate professor, Mount Sinai. Prof. Dubra had built a state-of-the-art AO-SLO device for Richard Rosen, and Toco Chiu was a postdoctoral researcher at the time in charge of operating the device and interpreting its scans.

Figure 7 (left) shows the montage of a series of AO-SLO scans. The temporal half of the B-scan from Figure 6B is shown aligned with the blood vessels (red lines). On the OCT image in Figure 7 (right), regions of preserved RNFL bundles can be seen. The hyperreflective regions of the RNFL (yellow arrows) are preserved RNFL, while the darker regions (orange arrows) show regions of missing RNFL bundles. That is, wher-

ever we saw remaining bundles of axons or RNF on the AO-SLO scans, we also saw preserved RNF on the OCT. Dark zones on the AO-SLO scans, where the RNF was completely wiped out, correlated to gaping areas on the OCT. Importantly, the existing RNF bundles on the AO-SLO scans appeared as tiny hyperreflective regions on the OCT that a clinician might mistake for artifacts. The message from this comparison was clear; we are *not* making optimal clinical use of the OCT information if we ignore these images and just look at summary statistics.

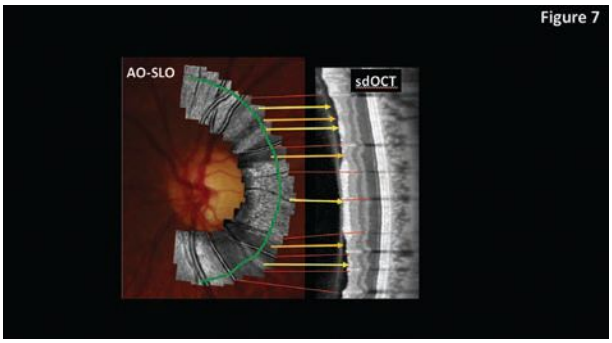

FIGURE 7. OCT AND AO-SLO. REGIONS OF PRESERVED RNFL BUNDLES CAN BE SEEN ON OCT B-SCANS
Comparing OCT scans to AO-SLO images revealed hyperreflective regions of preserved RNFL bundles.

LOCATION OF GLAUCOMATOUS DAMAGE

In 2012, to better understand the pattern of glaucomatous damage on OCTs, we obtained a series of OCT cube scans, centered on the macula and the optic disc, from glaucoma patients and age-matched controls.[6] From the macula scans, we obtained RNFL and RGC+ thickness data, and from the disc scans, we determined RNFL thickness. Data were averaged to obtain group RGC+ and RNFL thickness maps. When the averaged RNFL thickness map for healthy eyes was overlaid on a fundus photo, as in Figure 8A, it became obvious where most of the axons were located. To see where the largest loss in RNFL occurred, we subtracted the average RNFL map for the glaucomatous patients from those of the age-matched controls. Consistent with previous work,[7] we found that the superior and inferior quadrants showed the greatest loss in RNFL thickness. However, as Figure 8B shows, most of the loss occurred in the temporal half of the superior and inferior quadrants, which we called the superior (SVZ) and inferior (IVZ) vulnerability zones.

The same analysis was performed for the RGC+ thickness map obtained from cube scans centered on the fovea. In Figure 9A, the map showing the loss in RGC+ thickness in the same patients is superimposed on the photo and RNFL loss from Figure 8B. Figure 9B shows a schematic model we proposed to explain the pattern of macular damage and its relationship to the

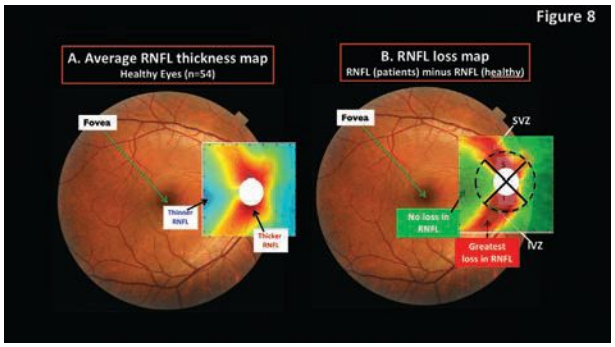

FIGURE 8. LOCATION OF DAMAGE
A. The RNFL thickness for the average of healthy controls. B. The loss in RNFL thickness for a group of patients with glaucoma.

IVZ (Figure 9B).[3,6,8,9] This work also documented that the 24-2 VF test pattern is suboptimal for detecting or following glaucomatous damage, and that macular damage is present even in the earliest stages of glaucoma.

DAMAGE AT THE MACULA

Until recently, the work of Harry Quigley and others[7] concluded that the superior and inferior quadrants were most vulnerable to glaucomatous damage at the optic disc. In general, this is true, although the areas of highest vulnerability are actually *the temporal halves* of the superior and inferior quadrants at the optic disc. Some other commonly held beliefs are that the temporal quadrant is much less affected, which is generally correct, and that the macular region is impacted last because the RGCs in this region send their axons to the less vulnerable temporal region, which is only partially correct. What we have shown is that RGCs in a large portion of the inferior macula send their axons into the most vulnerable part of the IVZ, as shown in our model in Figure 9B, not the temporal quadrant. The result is that macular damage is seen very early in the disease process in most eyes with glaucoma,[3,6,8,9] contrary to common belief.

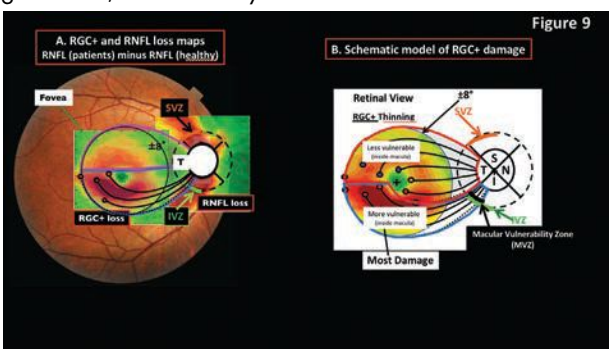

FIGURE 9. VULNERABILITY ZONES.
This figure shows how RGCs travel in glaucoma to the temporal halves of the inferior and superior quadrants.

We now know that arcuate defects near fixation are present in the earliest stages of glaucoma. Moreover, glaucoma, in addition to presenting with local defects

inside the MVZ, can have an early diffuse component across the macula.[3,8-11] It is this diffuse damage that can lead to vague patient complaints such as difficulty with extreme and low lighting, and diminished mobility in early glaucoma.[10]

COMPARING OCT ABNORMALITIES TO VF DEFECTS

Since no litmus test exists to definitively diagnose and stage glaucoma, clinicians typically compare patterns of change on VFs and OCT reports. The Keltner, Johnson, et al. classification[12] of VF defects (Figure 10), as detailed in the Ocular Hypertension Treatment Study, is commonly used for classifying abnormalities found on 24-2/30-2 VFs. (Note: the 30-2 has all the test locations of the 24-2 plus an outer ring of additional points.)

To compare VFs with OCT findings, it is necessary to produce a map of VF test locations corresponding to regions on the retina for an average eye, as illustrated by the map of 24-2 VF locations in Figure 10B.

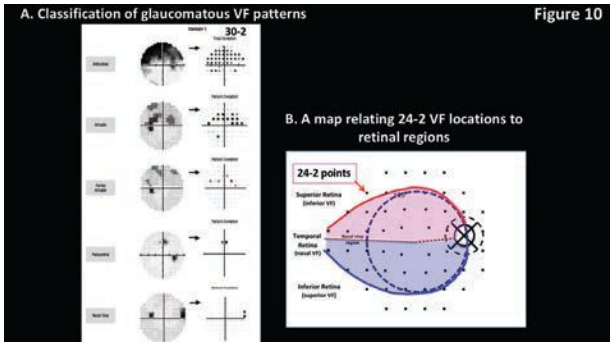

FIGURE 10. A MAP OF VF TEST POINTS
To compare VFs with OCT, it is necessary to produce a map of VF test points corresponding to regions on the retina for an average eye. Note: Figure 10A shows a classification scheme for a 30-2 report; the outer points are not included in the 24-2 map in panel B.

FIGURE 11 shows the regions from Figure 10B superimposed on the VFs from Figure 10A. This presentation underscores the fact that superior VF defects [second from top (arcuate) to bottom (nasal step) in Figure 11A] are due to damage in the IVZ (noted in the blue map regions). FIGURE 11B highlights in green the relatively small area where the damage occurred in the optic disc. Essentially, all of these upper VF defects are due to variations in a 45 to 90° region of the disc. The NSTIN scan in Figure 11C and schematic in Figure 11B illustrate that the VF defects within the blue region in Figure 11A are largely due to damage in a 45 to 90° region.

It stands to reason that since local RFNL damage on OCTs can vary in location, depth, width, and homogeneity,[3] and can frequently affect the macula,[3,6,8,9] we should expect VF defects to also exhibit a wide variety of patterns tending to occur at the macula.[3] This is

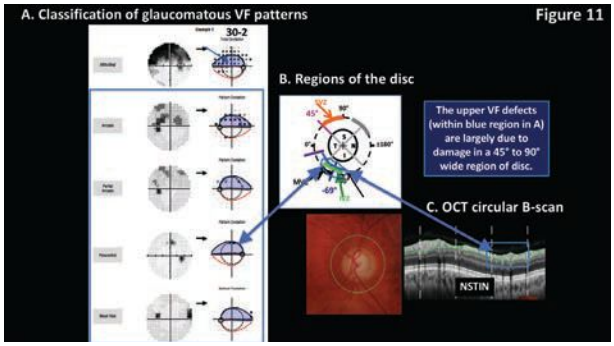

FIGURE 11. A SMALL REGION OF DAMAGE GENERATES A VARIETY OF FIELDS.
The upper VF defects for these five patients were largely due to damage in a 45- to 90-degree-wide region of optic disc, and primarily in a 45-degree segment.

illustrated in Figure 12, where the VFs and OCT scans of five patient are compared. The implication here is that VF classification schemes, such as those in Figures 10A and 11A, are a simplification of what is really a large range of VF defects.[3]

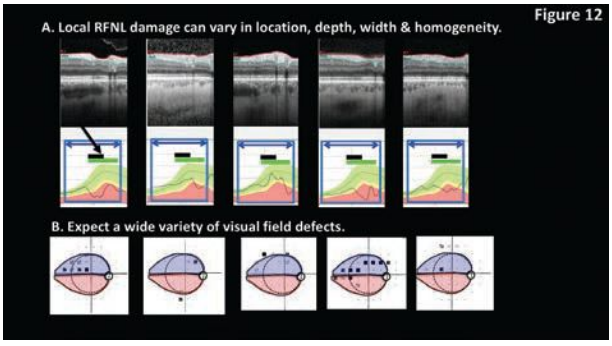

FIGURE 12. VF AND OCT DAMAGE IS DIVERSE & FREQUENTLY INCLUDES THE MACULA
The comparison of VF and OCT maps from five patients illustrates the wide patterns of damage seen on both, as well as the fact that the damage typically includes the macula; the black horizontal bar is the MVZ (black arrow).

In general, these comparisons of patterns of damage seen on VF deviation maps and OCT images have important clinical lessons.[3] First, the 24-2 VF test locations poorly sample the macular region, and, thus, the 24-2 and 30-2 VFs can miss or underestimate macular damage.[8,9,13–20] My colleague Dr. Gus De Moraes and I have been advising clinicians for several years that if there's reason to do a VF, there's a reason to do a 10-2 as well as a 24-2 VF, and if there's a reason to do OCT, it's essential to obtain a cube scan of the macula, not just the RNFL and disc, along with RGC+ thickness and probability maps.[1,2]

THE OCT REPORT

Since the clinician's diagnosis and understanding about a patients' glaucomatous damage are influenced by their understanding of the OCT, the commercial

OCT glaucoma reports available in OCT instruments are of utmost importance.

Based upon our experience with interpreting OCT scans and reports for clinicians, we created a one-page report of OCT findings to help clinicians detect and understand glaucomatous damage.[3,21] An example of our report is shown in Figure 13. For more details about interpreting this report, view lectures on my website at: https://hoodvisualscience.psychology.columbia.edu/videos

In simplest terms, the report is based upon four principles or rules:

Rule 1: A circumpapillary B-scan image should be examined for the presence of glaucomatous damage and/or segmentation errors. This image should be large enough and of sufficient quality so that local details can be visualized. For example, in the case of the B-scan in Figure 14 (left panel), the RNFL segmentation (green lines) looks correct, and local damage can be seen as well (red arrow).

Rule 2: Both GCL and RNFL probability/deviation maps are essential. Look for patterns (typically arcuates) of abnormal regions that are consistent with glaucoma. The RNFL probability map is particularly important for identifying these patterns. See, for example, the clear arcuate on the RNFL probability map in Figure 14 (upper right corner of right panel).

Rule 3: Assess topographical agreement of glaucomatous damage within the report. If the abnormal regions on the probability maps are due to glaucoma, as opposed to artifacts, then there should be topographical agreement with the abnormal regions in other parts of the report. For example, in Figure 15 (left panel), the red arrows point to the same topographical location, and the black arrows are locations in a corresponding arcuate region of damage. By asking for conformation within the report, the clinician can more easily confirm damage and rule out artifacts.

Rule 4: For comparisons to VFs, use the probability/deviations maps from 24-2 AND 10-2 VFs. Do not use summary metrics such as mean deviation (MD), pattern standard deviation (PSD) or glaucoma hemifield test (GHT), or OCT metrics like global or sector RNFL thickness.[1,2] Instead, directly compare abnormal regions seen on VFs with abnormal regions seen on RNFL and RGC probability maps.[3,22,23]

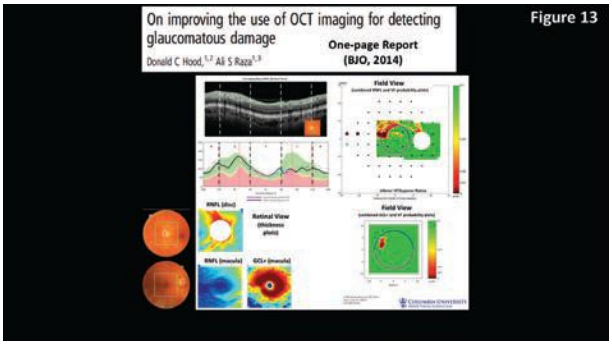

FIGURE 13. INTERNAL OCT LAB REPORT
A one-page report of OCT findings to help clinicians understand and diagnose glaucomatous damage is shown. It is based upon four rules.

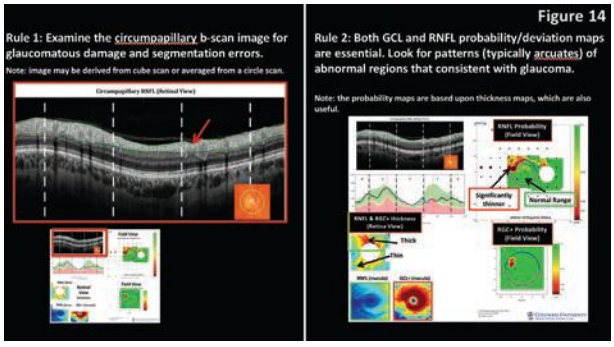

FIGURE 14. INTERNAL OCT LAB REPORT RULES 1 AND 2.

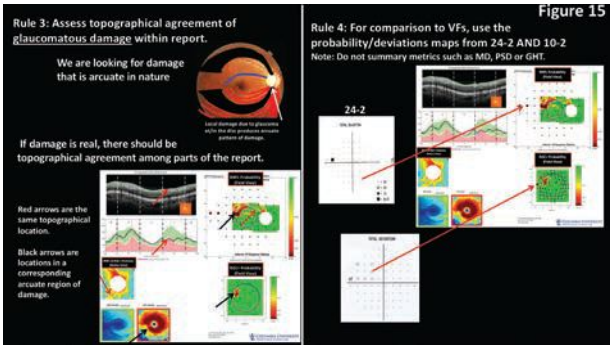

FIGURE 15. INTERNAL OCT LAB REPORT RULES 3 AND 4.

DEBUNKING MYTHS & THE FUTURE OF OCT

Many clinicians are taught that OCT is not useful for eyes with high myopia and/or advanced glaucoma. This is only true if one depends strictly on summary metrics, such as global or sector RNF thickness. In fact, contrary to popular opinion, we have found that glaucomatous damage in many, if not most, eyes with high myopia can be detected on OCT by experienced readers.[24] In addition, we have used OCT to understand glaucomatous damage and detect progression in eyes with advanced glaucoma.[25,26] All this is possible today with the reports and methods described in this lecture and on my website.

Despite our progress, we know that the OCT reports described here can be further improved. Current work is focusing on developing interactive versions and topographical models to aid the clinician,[4] as well as expanding these reports to allow for the progression of glaucoma to be more easily identified.[27] The goal is to give clinicians more information and greater confidence in their decisions, so they can better manage patients with, or at risk for, glaucoma.

Dr. Hood, the James F. Bender Professor of Psychology and Professor of Ophthalmic Science (in Ophthalmology), has been a member of the Columbia University faculty since 1969, and he has won all three of its major teaching awards.

1. Hood DC, De Moraes CG. Challenges to the Common Clinical Paradigm for Diagnosis of Glaucomatous Damage With OCT and Visual Fields. Invest Ophthalmol Vis Sci. 2018;59(2):788-91.
2. Hood DC, De Moraes CG. Four Questions for Every Clinician Diagnosing and Monitoring Glaucoma. J Glaucoma. 2018;27(8):657-64.
3. Hood DC. Improving our understanding, and detection, of glaucomatous damage: An approach based upon optical coherence tomography (OCT). Prog Retin Eye Res. 2017;57:46-75.
4. Hood DC, Zemborain ZZ, Tsamis E, De Moraes CG. Improving the Detection of Glaucoma and Its Progression: A Topographical Approach. J Glaucoma. 2020;29(8):613-21.
5. Hood DC, Chen MF, Lee D, et al. Confocal Adaptive Optics Imaging of Peripapillary Nerve Fiber Bundles: Implications for Glaucomatous Damage Seen on Circumpapillary OCT Scans. Transl Vis Sci Technol. 2015;4(2):12.
6. Hood DC, Raza AS, De Moraes CG, et al. The Nature of Macular Damage in Glaucoma as Revealed by Averaging Optical Coherence Tomography Data. Transl Vis Sci Technol. 2012;1(1):3-3.
7. Quigley HA, Addicks EM. Regional differences in the structure of the lamina cribrosa and their relation to glaucomatous optic nerve damage. Arch Ophthalmol Chic Ill 1960. 1981;99(1):137-43.
8. Hood DC, Raza AS, De Moraes CG, et al. Initial Arcuate Defects within the Central 10 Degrees in Glaucoma. Invest Ophthalmol Vis Sci. 2011;52(2):940-6.
9. Hood DC, Raza AS, De Moraes CG, et al. Glaucomatous damage of the macula. Prog Retin Eye Res. 2013;32:1-21.
10. Blumberg DM, Liebmann JM, Hirji SH, Hood DC. Diffuse Macular Damage in Mild to Moderate Glaucoma Is Associated With Decreased Visual Function Scores Under Low Luminance Conditions. Am J Ophthalmol. 2019;208:415-20.
11. Hood DC, Slobodnick A, Raza AS, De Moraes CG, et al. Early Glaucoma Involves Both Deep Local, and Shallow Widespread, Retinal Nerve Fiber Damage of the Macular Region. Invest Ophthalmol Vis Sci. 2014;55(2):632-49.
12. Keltner JL, Johnson CA, Cello KE, et al. Classification of visual field abnormalities in the ocular hypertension treatment study. Arch Ophthalmol Chic Ill 1960. 2003;121(5):643-50.
13. Langerhorst CT, Carenini LL, Bakker D, Det al. Measurements for description of very early glaucomatous field defects. In: International Perimetric Society, Meeting, Wall M, Heijl A, eds. Perimetry Update, 1996/1997: Proceedings of the XIIth International Perimetric Society Meeting, Würzburg, Germany, June 4-8, 1996. Kugler Publications; Distributor for the U.S.A. and Canada, DEMOS; 1997:67-73.
14. Schiefer U, Papageorgiou E, Sample PA, et al. Spatial pattern of glaucomatous visual field loss obtained with regionally condensed stimulus arrangements. Invest Ophthalmol Vis Sci. 2010;51(11):5685-9.
15. Traynis I, De Moraes CG, Raza AS, Liebmann JM, Ritch R, Hood DC. The Prevalence and Nature of Early Glaucomatous Defects in the Central 10° of the Visual Field. JAMA Ophthalmol. 2014;132(3):291-7.
16. Park H-YL, Hwang B-E, Shin H-Y, et al. Clinical Clues to Predict the Presence of Parafoveal Scotoma on Humphrey 10-2 Visual Field Using a Humphrey 24-2 Visual Field. Am J Ophthalmol. 2016;161:150-9.
17. Sullivan-Mee M, Karin Tran MT, Pensyl D, et al. Prevalence, Features, and Severity of Glaucomatous Visual Field Loss Measured With the 10-2 Achromatic Threshold Visual Field Test. Am J Ophthalmol. 2016;168:40-51.
18. Jung KI, Kim EK, Park CK. Usefulness of frequency doubling technology perimetry 24-2 in glaucoma with parafoveal scotoma. Medicine (Baltimore). 2017;96(24).
19. Roberti G, Manni G, Riva I, et al. Detection of central visual field defects in early glaucomatous eyes: Comparison of Humphrey and Octopus perimetry. PloS One. 2017;12(10):e0186793.
20. De Moraes CG, Hood DC, Thenappan A, et al. 24-2 Visual Fields Miss Central Defects Shown on 10-2 Tests in Glaucoma Suspects, Ocular Hypertensives, and Early Glaucoma. Ophthalmology. 2017;124(10):1449-56.
21. Hood DC, Raza AS. On improving the use of OCT imaging for detecting glaucomatous damage. Br J Ophthalmol. 2014;98 Suppl 2:ii1-9.
22. Tsamis E, Bommakanti NK, Sun A, Thakoor KA, Moraes CGD, Hood DC. An Automated Method for Assessing Topographical Structure–Function Agreement in Abnormal Glaucomatous Regions. Transl Vis Sci Technol. 2020;9(4):14-14.
23. Hood DC, Tsamis E, Bommakanti NK, et al. Structure-Function Agreement Is Better Than Commonly Thought in Eyes With Early Glaucoma. Invest Ophthalmol Vis Sci. 2019;60(13):4241-8.
24. Zemborain ZZ, Jarukasetphon R, Tsamis E, De Moraes CG, Ritch R, Hood DC. Optical Coherence Tomography Can Be Used to Assess Glaucomatous Optic Nerve Damage in Most Eyes With High Myopia. J Glaucoma. 2020;29(10):833-45.
25. Lee S, Joiner D, Tsamis E, et al. OCT Circle Scans Can Be Used to Study Many Eyes with Advanced Glaucoma. Ophthalmol Glaucoma. 2019;2(3):130-5.
26. Thenappan A, Tsamis E, Zemborain ZZ, et al. Detecting Progression in Advanced Glaucoma: Are OCT Global Metrics Viable Measures? Optom Vis Sci. 2021. In press.
27. Hood DC, Melchior B, Tsamis E, Liebmann J, De Moraes CG. Did the OCT show progression since the last visit? J Glaucoma. 2021; Jan 7. [Epub ahead of print].

ANTERIOR SEGMENT

Foundations of Glaucoma in the Anterior Segment

Thomas F. Freddo, OD, PhD, FAAO

To fully comprehend how glaucoma causes progressive and vision-threatening damage over time, it's essential to understand the biology that occurs in and around the anterior segment, and how it is altered with disease, including both aqueous inflow and outflow.

Shining a light on how dysregulation of natural processes can create circumstances leading to aqueous humor flow obstruction, elevated intraocular pressure (IOP) and damage to retinal ganglion cells illuminates how therapies can potentially interrupt the pathological processes of glaucoma within the anterior and posterior segment. With these fundamental insights, clinicians are offered an important guidepost for how best to approach and manage their patients' disease.

AQUEOUS INFLOW

Aqueous humor is a clear fluid, secreted across the ciliary epithelium, which provides nutrients to the avascular tissues of the anterior segment of the eye, and which contains various elements that sustain the immunosuppressive environment of the anterior chamber.[1]

Aqueous production (inflow) is the result of two inter-related processes: ultrafiltration through the microvasculature of the ciliary body stroma, and aqueous secretion by the pigmented (PCEs) and non-pigmented ciliary epithelial cells (NPCEs). Aqueous humor, once secreted from the ciliary body into the posterior chamber, flows through the pupil into the anterior chamber, where a convection current driven by the temperature difference between the warm iris and cooler cornea circulates it to provide nutrients and remove waste products.

Aqueous humor is secreted exclusively by the tips of the ciliary processes—epithelium-covered ridges containing a fibrovascular core. These ridges are arranged radially around the lens in the pars plicata

region of the ciliary body, and each ridge is known as a "ciliary process." Posterior to the pars plicata region, on the inner surface of the pars plana region of the ciliary body, a carpet of zonular fibers that originate between ciliary epithelial cells near the ora seratta, extend anteriorly. When they reach the posterior edge of the pars plicata, they form bundles that channel into the valleys between the ciliary processes, attaching again before changing direction to reach the lens capsule. The ciliary body functions as a kind of exocrine gland, with its secretory epithelial surface underlain by a fibrovascular stroma containing blood vessels, autonomic nerves, and intercellular junctions that regulate and control secretions.

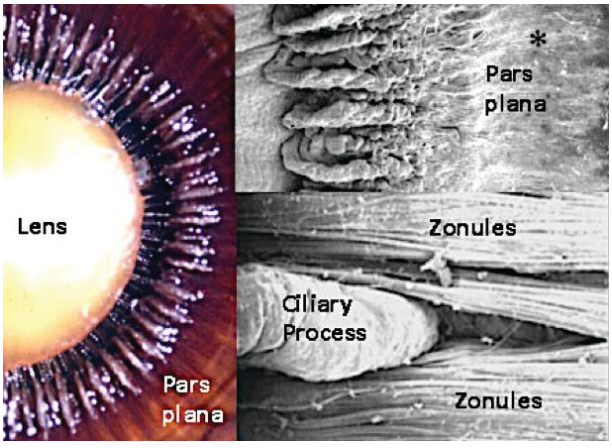

FIGURE 1. PARS PLICATA AND BEYOND
(Left) In a macrophotograph of the ciliary body and lens viewing forward from the vitreous chamber, fin-like ridges of the ciliary processes of the pars plicata and the surrounding ring of the pars plana can be seen. (Top right) A scanning electron micrograph shows a view of the ciliary processes. (Bottom right) The posterior edge of one ciliary process and the channeling of the carpet of zonular fibers into the valleys between ciliary processes is depicted. *Images: Thomas F. Freddo, OD, PhD*

Aqueous humor is produced at a rate of approximately 3 microliters (µl) per minute, although some researchers argue the rate is about twice that, with the additional volume getting lost to diffusional exchange into and out of the vitreous.[2] Aqueous humor secreted into the posterior chamber enters the anterior chamber exclusively through the pupil, and has to constantly circulate to deliver its nutrients to the avascular tissues (cornea, lens, and trabecular meshwork) and then carry away their waste. It circulates in a convection current driven by temperature differences in the anterior chamber—rising along the warmer iris and falling along the inner surface of the cooler cornea.

The fluid contains glucose, amino acids, locally made immunoregulatory proteins, and just enough oxygen to sustain anaerobic metabolism. Aqueous also contains plasma constituents, including the iron-scavenging protein transferrin and the antioxidant ascorbate, both of which are actively transported into the aqueous and found at higher levels in aqueous than in plasma.[1]

A very low, but constant, level of plasma proteins also can be found in aqueous humor samples obtained from the anterior chamber. For decades, researchers wondered where this protein originated, given that the iris vessels and ciliary epithelium contain tight junctions between their cells and are known not to leak plasma proteins in the uninflamed eye.

In a series of *in vivo* studies conducted over about 20 years, it was found that the plasma-derived protein in aqueous humor in the anterior chamber is not a part of aqueous humor as it is secreted into the posterior chamber. The source of the plasma protein is the

CLEARING UP MYTHS ABOUT 2 GLAUCOMA DRUGS & THE BLOOD AQUEOUS BARRIER

Pilocarpine is a muscarinic cholinergic agonist historically used to reduce IOP in ocular hypertension, primary open-angle glaucoma (POAG), and angle-closure glaucoma (ACG) in advance of surgery, although it's less commonly used today for long-term glaucoma management due to its side effect profile. The package insert on pilocarpine has traditionally noted that the drug breaks down the blood aqueous barrier, conveniently serving to explain the commonly seen transient flare post-instillation in patients during examination. After my team completed studies in normal human subjects identifying the true source of plasma-derived protein in aqueous humor,[3] we replicated the research with pilocarpine and found that the drug did not breach the blood aqueous barrier.[6] No leakage of the intravenously injected tracer was found in the posterior chamber using high-resolution MRI. We know that the protein pathway for delivery of plasma proteins to the anterior chamber also puts a reservoir of these proteins into the iris stroma. When pilocarpine is instilled and produces a strong miosis that thins the iris stroma, some of the protein reservoir is squeezed into the anterior chamber, creating the transient flare known to occur after pilocarpine. But there is no increased permeability of the blood aqueous barrier.[6]

Our documentation of this novel protein pathway in human volunteers using MRI also explained the flare that follows the use of aqueous humor suppressants such as timolol. Prior to our documentation of this protein pathway, it was again assumed that the only way for protein levels to rise in the aqueous was by breakdown of the blood aqueous barrier. But our documentation that aqueous humor and the plasma protein within in it enter semi-independently means that if we suppress aqueous secretion by 50%, as commonly occurs using timolol, only half the aqueous humor will be available to dilute the continued plasma protein entry into the anterior chamber via the iris root.[7] The result is the appearance of flare that is purely due to this concentration effect—again with no breakdown of the blood-aqueous barrier as was previously believed.

permeable vessels of the ciliary body stroma, through which the plasma protein enters the anterior chamber directly, and diffuses forward toward the ciliary body band, filling the iris stroma and secondarily diffusing into the anterior chamber.[3-5] This protein never enters the posterior chamber in the normal eye.

Until this discovery, theories held that any increase in aqueous humor protein concentration (i.e., clinical flare) must be the result of a breakdown of the blood-aqueous barrier. A series of studies showed that aqueous humor protein concentration could also increase through a concentration effect that did not involve breakdown of the blood-aqueous barrier.

VASCULATURE IN THE CILIARY PROCESSES

To understand aqueous humor production, it's necessary to first understand the anatomy of the ciliary processes. Each ciliary process is fed by two sets of vessels, which originate from the major circle of the iris. The vessels emerging from the posterior surface of the major circle run less deeply within each process and give rise to non-fenestrated capillaries that allow for movement of fluid and ions, but not plasma proteins.[8] The vessels that emerge from the anterior surface of the major circle give rise to the marginal capillaries that pass into the deepest part of the ciliary processes at their tips.[8] These vessels exhibit fenestrated capillaries that leak ions, fluid, and plasma proteins. Some of the protein diffuses through the ciliary body stroma and the iris root, into the anterior but not the posterior chamber, because protein diffusion is blocked by tight junctions (zonulae occludentes) between ciliary epithelial cells that seal the intercellular path for diffusion from the ciliary body stroma toward the posterior chamber.[9] The marginal capillaries release an ultrafiltrate of fluid, ions, and plasma protein into the ciliary body stroma, providing the source material from which aqueous is secreted.

The ridges of ciliary processes are covered on both sides by two layers of epithelial cells that work in concert to secrete aqueous humor, using fluid and ions from the pool of ultrafiltrate in the ciliary body stroma. Both layers are named for their content of pigment. One of these two layers contains pigment (pigmented ciliary epithelium [PCE]) and faces the ciliary body stroma. The other contains no pigment (non-pigmented ciliary epithelium [NPCE]) and faces the posterior chamber. The ultrafiltrate in the ciliary body stroma contains about three-quarters of the plasma protein concentration of that found in the blood; yet, there is no non-specific diffusion of this plasma protein into the posterior chamber. Maintaining such a severe gradient in protein concentration between the ciliary body stroma (74%) and the posterior chamber (0%) requires a strong barrier between these compartments. Such a blockade occurs between adjacent NPCEs at their apices, and is known as a "tight junction," or zonula occludens.[9] This junction forms a continuous belt, sealing the paracellular space between each cell and every other cell that it touches. Its disruption in the ciliary epithelium and within the walls of iris blood vessels allows protein to leak into the aqueous humor in anterior uveitis, producing clinically observable flare.[10]

Gap junctions join the layers of the ciliary epithelia to each other, and join cells within each layer. These focal junctions convey ions and even second messenger molecules from PCEs to NPCEs, and transmit electrical currents enabling metabolic and electrotonic communication between cells. This communication allows for the movement of ions and for coordination of the ciliary epithelium in the secretion of aqueous humor. To hold the cells of each layer together and to hold the two cell layers to each other, two types of intercellular junctions are designed for cellular adhesion. The zonula adherens runs around the circumference of the cell near the tight junction, and numerous desmosomes serve as "spot welds," joining adjacent cells together and anchoring the cytoskeletons of adjacent cells to one another for structural stability.[9]

AQUEOUS HUMOR PRODUCTION

The time window of highest aqueous humor production is debated in the literature, but most accounts agree that production drops by about 50% at night.[11-13] That is why the beta-blocker timolol, which is known to reduce aqueous production by 50%, didn't have an additive effect on aqueous secretion at night—because it reduced production through the same mechanism and by about the same magnitude as the normal diurnal curve.[7]

The traditional physiological model used to understand how ciliary epithelial layers move fluid and ions from the ultrafiltrate to secrete aqueous humor is found in the Diamond-Bossert model of standing gradient osmotic flow. In the simplest form of this model, sodium and chloride ions are taken in from the ultrafiltrate in the ciliary body stroma by the PCE, conveyed to the NPCE cells via gap junction channels, and pumped into the cleft between adjacent NPCE cells, by a sodium-potassium ATPase pump, serving to make this space hypertonic and drawing water into the cleft as an osmotic water flux to dilute this ion concentration. The tight junction sealing the NPCE cells together at their apices restricts flow that enters this narrow cleft from moving toward the PCEs and directs it into the posterior chamber, yielding aqueous humor.

The intake of sodium and chloride ions by the pigmented ciliary epithelium is critical and depends upon a continually replenished supply of hydrogen ions and

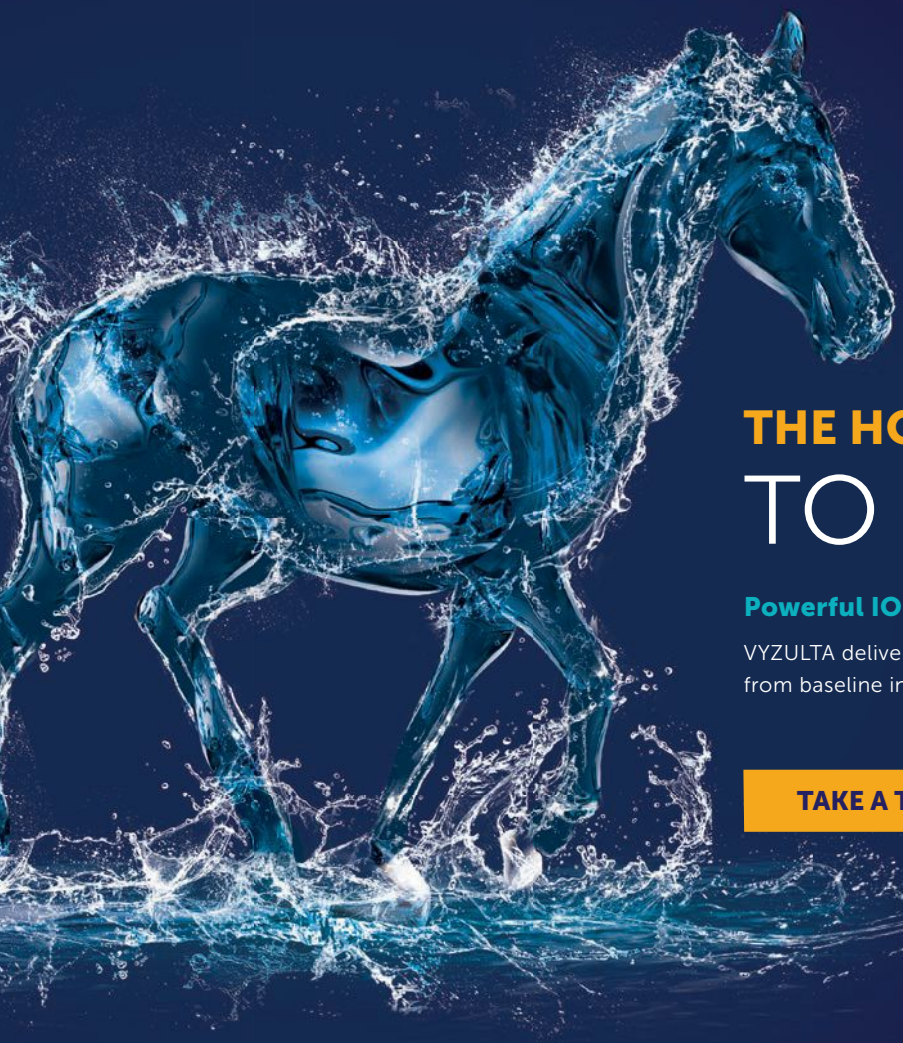

VYZULTA®
(latanoprostene bunod ophthalmic solution), 0.024%

THE HORSEPOWER YOU NEED TO LOWER IOP

Powerful IOP reduction with excellent tolerability[1,2]

VYZULTA delivered **up to 9.1 mmHg mean IOP reduction** from baseline in pivotal trials.[1,2*]

TAKE A TEST RIDE AT VYZULTAHCP.COM

*Pivotal study designs: Two Phase 3, randomized, multicenter, parallel-group studies, APOLLO and LUNAR, evaluating noninferiority of once-daily VYZULTA vs twice-daily timolol maleate 0.5% in patients with open-angle glaucoma or ocular hypertension. Primary endpoint was IOP measured at 9 assessment time points in study eye. APOLLO (VYZULTA, n=284; timolol, n=133) and LUNAR (VYZULTA, n=278; timolol, n=136).[2,3]

INDICATION

VYZULTA® (latanoprostene bunod ophthalmic solution), 0.024% is indicated for the reduction of intraocular pressure (IOP) in patients with open-angle glaucoma or ocular hypertension.

IMPORTANT SAFETY INFORMATION

- Increased pigmentation of the iris and periorbital tissue (eyelid) can occur. Iris pigmentation is likely to be permanent
- Gradual changes to eyelashes, including increased length, increased thickness, and number of eyelashes, may occur. These changes are usually reversible upon treatment discontinuation
- Use with caution in patients with a history of intraocular inflammation (iritis/uveitis). VYZULTA should generally not be used in patients with active intraocular inflammation
- Macular edema, including cystoid macular edema, has been reported during treatment with prostaglandin analogs. Use with caution in aphakic patients, in pseudophakic patients with a torn posterior lens capsule, or in patients with known risk factors for macular edema
- There have been reports of bacterial keratitis associated with the use of multiple-dose containers of topical ophthalmic products that were inadvertently contaminated by patients
- Contact lenses should be removed prior to the administration of VYZULTA and may be reinserted 15 minutes after administration
- Most common ocular adverse reactions with incidence ≥2% are conjunctival hyperemia (6%), eye irritation (4%), eye pain (3%), and instillation site pain (2%)

For more information, please see Brief Summary of full Prescribing Information on adjacent page.

References: 1. VYZULTA Prescribing Information. Bausch & Lomb Incorporated. **2.** Weinreb RN, Scassellati Sforzolini B, Vittitow J, Liebmann J. Latanoprostene bunod 0.024% versus timolol maleate 0.5% in subjects with open-angle glaucoma or ocular hypertension: the APOLLO study. *Ophthalmology.* 2016;123(5):965-973. **3.** Medeiros FA, Martin KR, Peace J, Scassellati Sforzolini B, Vittitow JL, Weinreb RN. Comparison of latanoprostene bunod 0.024% and timolol maleate 0.5% in open-angle glaucoma or ocular hypertension: the LUNAR study. *Am J Ophthalmol.* 2016;168:250-259.

BAUSCH + LOMB

BRIEF SUMMARY OF PRESCRIBING INFORMATION

This Brief Summary does not include all the information needed to use VYZULTA safely and effectively. See full Prescribing Information for VYZULTA.

VYZULTA® (latanoprostene bunod ophthalmic solution), 0.024%, for topical ophthalmic use.

Initial U.S. Approval: 2017

1 INDICATIONS AND USAGE

VYZULTA® (latanoprostene bunod ophthalmic solution) 0.024% is indicated for the reduction of intraocular pressure (IOP) in patients with open-angle glaucoma or ocular hypertension.

4 CONTRAINDICATIONS

None

5 WARNINGS AND PRECAUTIONS

5.1 Pigmentation

VYZULTA® (latanoprostene bunod ophthalmic solution), 0.024% may cause changes to pigmented tissues. The most frequently reported changes with prostaglandin analogs have been increased pigmentation of the iris and periorbital tissue (eyelid).

Pigmentation is expected to increase as long as latanoprostene bunod ophthalmic solution is administered. The pigmentation change is due to increased melanin content in the melanocytes rather than to an increase in the number of melanocytes. After discontinuation of VYZULTA, pigmentation of the iris is likely to be permanent, while pigmentation of the periorbital tissue and eyelash changes are likely to be reversible in most patients. Patients who receive prostaglandin analogs, including VYZULTA, should be informed of the possibility of increased pigmentation, including permanent changes. The long-term effects of increased pigmentation are not known.

Iris color change may not be noticeable for several months to years. Typically, the brown pigmentation around the pupil spreads concentrically towards the periphery of the iris and the entire iris or parts of the iris become more brownish. Neither nevi nor freckles of the iris appear to be affected by treatment. While treatment with VYZULTA® (latanoprostene bunod ophthalmic solution), 0.024% can be continued in patients who develop noticeably increased iris pigmentation, these patients should be examined regularly *[see Patient Counseling Information (17) in full Prescribing Information]*.

5.2 Eyelash Changes

VYZULTA may gradually change eyelashes and vellus hair in the treated eye. These changes include increased length, thickness, and the number of lashes or hairs. Eyelash changes are usually reversible upon discontinuation of treatment.

5.3 Intraocular Inflammation

VYZULTA should be used with caution in patients with a history of intraocular inflammation (iritis/uveitis) and should generally not be used in patients with active intraocular inflammation as it may exacerbate this condition.

5.4 Macular Edema

Macular edema, including cystoid macular edema, has been reported during treatment with prostaglandin analogs. VYZULTA should be used with caution in aphakic patients, in pseudophakic patients with a torn posterior lens capsule, or in patients with known risk factors for macular edema.

5.5 Bacterial Keratitis

There have been reports of bacterial keratitis associated with the use of multiple-dose containers of topical ophthalmic products. These containers had been inadvertently contaminated by patients who, in most cases, had a concurrent corneal disease or a disruption of the ocular epithelial surface.

5.6 Use with Contact Lens

Contact lenses should be removed prior to the administration of VYZULTA because this product contains benzalkonium chloride. Lenses may be reinserted 15 minutes after administration.

6 ADVERSE REACTIONS

The following adverse reactions are described in the Warnings and Precautions section: pigmentation (5.1), eyelash changes (5.2), intraocular inflammation (5.3), macular edema (5.4), bacterial keratitis (5.5), use with contact lens (5.6).

6.1 Clinical Trials Experience

Because clinical trials are conducted under widely varying conditions, adverse reaction rates observed in the clinical trials of a drug cannot be directly compared to rates in the clinical trials of another drug and may not reflect the rates observed in practice.

VYZULTA was evaluated in 811 patients in 2 controlled clinical trials of up to 12 months duration. The most common ocular adverse reactions observed in patients treated with latanoprostene bunod were: conjunctival hyperemia (6%), eye irritation (4%), eye pain (3%), and instillation site pain (2%). Approximately 0.6% of patients discontinued therapy due to ocular adverse reactions including ocular hyperemia, conjunctival irritation, eye irritation, eye pain, conjunctival edema, vision blurred, punctate keratitis and foreign body sensation.

8 USE IN SPECIFIC POPULATIONS

8.1 Pregnancy

Risk Summary

There are no available human data for the use of VYZULTA during pregnancy to inform any drug associated risks.

Latanoprostene bunod has caused miscarriages, abortion, and fetal harm in rabbits. Latanoprostene bunod was shown to be abortifacient and teratogenic when administered intravenously (IV) to pregnant rabbits at exposures ≥ 0.28 times the clinical dose. Doses ≥ 20 µg/kg/day (23 times the clinical dose) produced 100% embryofetal lethality. Structural abnormalities observed in rabbit fetuses included anomalies of the great vessels and aortic arch vessels, domed head, sternebral and vertebral skeletal anomalies, limb hyperextension and malrotation, abdominal distension and edema. Latanoprostene bunod was not teratogenic in the rat when administered IV at 150 mcg/kg/day (87 times the clinical dose) *[see Data]*.

The background risk of major birth defects and miscarriage for the indicated population is unknown. However, the background risk in the U.S. general population of major birth defects is 2 to 4%, and of miscarriage is 15 to 20%, of clinically recognized pregnancies.

Data

Animal Data

Embryofetal studies were conducted in pregnant rabbits administered latanoprostene bunod daily by intravenous injection on gestation days 7 through 19, to target the period of organogenesis. The doses administered ranged from 0.24 to 80 mcg/kg/day. Abortion occurred at doses ≥ 0.24 mcg/kg/day latanoprostene bunod (0.28 times the clinical dose, on a body surface area basis, assuming 100% absorption). Embryofetal lethality (resorption) was increased in latanoprostene bunod treatment groups, as evidenced by increases in early resorptions at doses ≥ 0.24 mcg/kg/day and late resorptions at doses ≥ 6 mcg/kg/day (approximately 7 times the clinical dose). No fetuses survived in any rabbit pregnancy at doses of 20 mcg/kg/day (23 times the clinical dose) or greater. Latanoprostene bunod produced structural abnormalities at doses ≥ 0.24 mcg/kg/day (0.28 times the clinical dose). Malformations included anomalies of sternum, coarctation of the aorta with pulmonary trunk dilation, retroesophageal subclavian artery with absent brachiocephalic artery, domed head, forepaw hyperextension and hindlimb malrotation, abdominal distention/edema, and missing/fused caudal vertebrae.

An embryofetal study was conducted in pregnant rats administered latanoprostene bunod daily by intravenous injection on gestation days 7 through 17, to target the period of organogenesis. The doses administered ranged from 150 to 1500 mcg/kg/day. Maternal toxicity was produced at 1500 mcg/kg/day (870 times the clinical dose, on a body surface area basis, assuming 100% absorption), as evidenced by reduced maternal weight gain. Embryofetal lethality (resorption and fetal death) and structural anomalies were produced at doses ≥ 300 mcg/kg/day (174 times the clinical dose). Malformations included anomalies of the sternum, domed head, forepaw hyperextension and hindlimb malrotation, vertebral anomalies and delayed ossification of distal limb bones. A no observed adverse effect level (NOAEL) was established at 150 mcg/kg/day (87 times the clinical dose) in this study.

8.2 Lactation

Risk Summary

There are no data on the presence of VYZULTA in human milk, the effects on the breastfed infant, or the effects on milk production. The developmental and health benefits of breastfeeding should be considered, along with the mother's clinical need for VYZULTA, and any potential adverse effects on the breastfed infant from VYZULTA.

8.4 Pediatric Use

Use in pediatric patients aged 16 years and younger is not recommended because of potential safety concerns related to increased pigmentation following long-term chronic use.

8.5 Geriatric Use

No overall clinical differences in safety or effectiveness have been observed between elderly and other adult patients.

13 NONCLINICAL TOXICOLOGY

13.1 Carcinogenesis, Mutagenesis, Impairment of Fertility

Latanoprostene bunod was not mutagenic in bacteria and did not induce micronuclei formation in the *in vivo* rat bone marrow micronucleus assay. Chromosomal aberrations were observed *in vitro* with human lymphocytes in the absence of metabolic activation.

Latanoprostene bunod has not been tested for carcinogenic activity in long-term animal studies. Latanoprost acid is a main metabolite of latanoprostene bunod. Exposure of rats and mice to latanoprost acid, resulting from oral dosing with latanoprost in lifetime rodent bioassays, was not carcinogenic.

Fertility studies have not been conducted with latanoprostene bunod. The potential to impact fertility can be partially characterized by exposure to latanoprost acid, a common metabolite of both latanoprostene bunod and latanoprost. Latanoprost acid has not been found to have any effect on male or female fertility in animal studies.

13.2 Animal Toxicology and/or Pharmacology

A 9-month toxicology study administered topical ocular doses of latanoprostene bunod to one eye of cynomolgus monkeys: control (vehicle only), one drop of 0.024% bid, one drop of 0.04% bid and two drops of 0.04% per dose, bid. The systemic exposures are equivalent to 4.2-fold, 7.9-fold, and 13.5-fold the clinical dose, respectively, on a body surface area basis (assuming 100% absorption). Microscopic evaluation of the lungs after 9 months observed pleural/subpleural chronic fibrosis/inflammation in the 0.04% dose male groups, with increasing incidence and severity compared to controls. Lung toxicity was not observed at the 0.024% dose.

U.S. Patent Numbers: 7,273,946; 7,629,345; 7,910,767; 8,058,467.

Distributed by:

Bausch + Lomb, a division of

Bausch Health US, LLC

Bridgewater, NJ 08807 USA

Based on 9612403 (Folded), 9612303 (Flat) 5/2019

VYZ.0109.USA.20 Issued: 5/2020

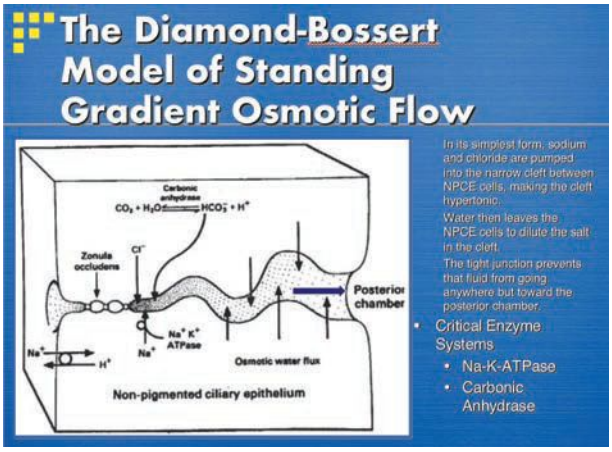

FIGURE 2. DIAMOND-BOSSERT MODEL OF STANDING GRADIENT OSMOTIC FLOW

A simplified way to understand how aqueous humor is produced is found in the Diamond-Bossert Model of Standing Gradient Osmotic Flow.

bicarbonate ions in the cytoplasm. These two ions must be produced and shipped out of the cell in exchange for the entry of Na^+ and Cl^- ions. The primary role of carbonic anhydrase in the production of aqueous humor is to cleave cytoplasmic carbonic acid (made from CO_2 and water) into H^+ and $HCO3^-$, to provide these ions for exchange. By inhibiting carbonic anhydrase, sodium and chloride uptake are reduced and aqueous humor production is inhibited, reducing IOP.

AQUEOUS OUTFLOW

Total aqueous outflow is the combination of fluid exiting the trabecular meshwork, through the conventional outflow pathway via Schlemm's canal to the episcleral veins, and that leaving the uveoscleral outflow pathway. Conventional outflow through the trabecular meshwork is pressure-dependent, whereas uveoscleral outflow is relatively pressure independent except at very low pressures.

Conventional aqueous humor outflow is a passive flow along a downhill pressure gradient from the anterior chamber to the episcleral veins. For aqueous humor to leave the eye via the conventional route, IOP must be greater than episcleral venous pressure (EVP). The data on whether EVP is elevated in POAG remains equivocal, but researchers at the Mayo Clinic are using newer technologies to address this question.[14]

Normal EVP averages 8 to 10 mmHg when a person is seated,[14] but it can be raised by clinical scenarios that obstruct venous outflow or involve arteriovenous malformations. Dilated episcleral vessels, with elevated IOP, may indicate a recent trauma. Other etiologies may result in venous obstruction such as hyperthyroidism, amyloidosis, congestive heart failure, hypercoagulability states, vasculitides, superior vena cava syndrome, or Sturge-Weber syndrome. Sturge-Weber is one condition in which the consensus seems to be the root cause of the associated rise in IOP is, indeed, EVP elevation.[15]

BETA-1&2 AND ALPHA-2 RECEPTORS

Some glaucoma medications alter aqueous humor production by stimulating or inhibiting adrenergic receptors on NPCEs. Beta-1 and -2, and alpha-2 adrenergic receptors, located on the membrane of the ciliary epithelial cells, are G-protein-linked receptors—intramembranous proteins linked to these surface receptors that send the message of activation to cascades of intracellular biochemical pathways and influence the rate of aqueous production. Different G-proteins can stimulate or inhibit these biochemical cascades. Beta-1 or -2 receptors are linked to stimulatory G-proteins, so if a molecule binds and activates them, activation of the G-protein occurs through phosphorylation by guanosine-5′-triphosphate (GTP) rather than adenosine triphosphate (ATP). The active G-protein then stimulates a cascade of events beginning with upregulation of adenyl cyclase, which in turn upregulates cyclic adenosine monophosphate. Cyclic adenosine monophosphate (cAMP), a "second messenger," then upregulates protein kinase A. Second messenger molecules can pass through gap junctions, causing surrounding cells to respond to receptor activation of one cell in order to create an amplified and coordinated effect. Through this mechanism, upregulation of protein kinase A will then occur in all surrounding cells. This prompts the final effect—increasing the speed at which a sodium potassium ATPase pump turns in the NPCE membrane, which increases sodium export and aqueous production, and, if outflow remains unchanged, leads to elevation of IOP.

Molecules that bind the beta receptor without causing G-protein activation inhibit the acceleration of aqueous production because the receptor is blocked, and are known as beta-blockers, a tool in the glaucoma armamentarium. Alpha-2 receptors affect the same cascade of pathways but in the opposite direction. When an alpha-2 receptor is bound and activated by an agonist, its G-protein is phosphorylated as well, but the activated G protein to which the alpha-2 receptor is linked is an inhibitory G-protein. As such, alpha-2 receptor binding and G-protein phosphorylation will down regulate adenyl cyclase. This leads to down regulation of cyclic AMP and protein kinase A, causing the sodium potassium ATPase pump to spin more slowly.

Thus, activation of beta-1 or -2 receptors increases aqueous production, and activation of alpha-2 receptors decreases aqueous production. Because they are different receptor systems that converge on a common pathway, combining the use of a beta-blocker and an alpha-agonist further reduces aqueous production and IOP in glaucoma.

CONVENTIONAL OUTFLOW PATHWAY ANATOMY

The conventional outflow pathway includes the trabecular meshwork, Schlemm's canal, the collector chan-

nels, and the multiple channels that weave through the limbal sclera to join the episcleral veins. From a functional standpoint, this pathway is often subdivided into a proximal and a distal portion. The proximal portion includes the trabecular meshwork and Schlemm's canal, while the distal portion includes the external collector channels and all of the small vessels weaving through the sclera to join the episcleral veins.

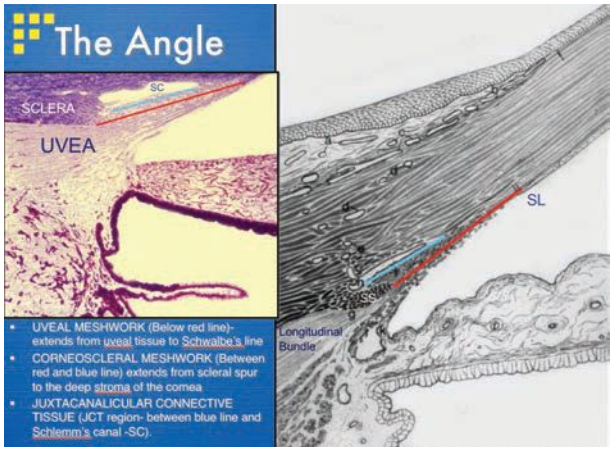

FIGURE3. CONVENTIONAL OUTFLOW PATHWAY.
The conventional outflow pathway includes the trabecular meshwork, Schlemm's canal, the collector channels, and the multiple channels that weave through the limbal sclera to join the episcleral veins. This pathway is often subdivided into a proximal and a distal portion.

THE PROXIMAL PORTION

Uveal Meshwork. The trabecular meshwork is traditionally divided into three areas, progressing from the anterior chamber toward Schlemm's canal. If an imaginary line is drawn from the scleral spur to Schwalbe's line, the portion of the trabecular meshwork that is internal to that line, extending from Schwalbe's line (the edge of Descemet's membrane) to the ciliary body and root of the iris, is termed the "uveal meshwork."

Corneoscleral Meshwork. On the other side of the red line, the portion of the meshwork that extends from the posterior lamellae of the corneal stroma to the scleral spur is termed the corneoscleral meshwork.

Both the uveal and corneoscleral meshwork are composed of branching and interconnecting avascular trabecular beams. Each has a structural central core of collagen and elastic tissue enveloped in a layer of trabecular endothelial cells. The main difference between the uveal and corneoscleral meshwork is the size of openings that provide the passageways for aqueous humor. In the uveal meshwork, the average size of the flow pathways is about 25 to 75 µm, whereas the average size of the flow pathways in the corneoscleral meshwork is 2 to 15 µm.[16]

Juxtacanalicular Connective Tissue. The third portion of the trabecular meshwork, which is deeper than the corneoscleral meshwork and resides along the inner wall of Schlemm's canal, is the juxtacanalicular connective tissue (JCT). The JCT has a unique architecture with no beams formed there, and is composed of an open connective tissue matrix of collagen, elastic tissue, and juxtacanalicular cells. The flow passages for aqueous humor are much smaller in this region, measuring 1 to 2µm.[16] Given the relatively large passageways for flow in the normal uveal and corneoscleral meshwork, neither is considered to contribute any measurable resistance of aqueous outflow.[17]

Schlemm's Canal. Schlemm's canal is composed of a single layer of endothelial cells resting on a "basement" membrane. Along the inner wall of the canal, this basement membrane is discontinuous, possibly as a result of the continuous flow of aqueous toward the canal washing it away. Because the inner wall represents a continuous cell barrier to the free flow of aqueous, it makes some contribution to outflow resistance. In response to pressure differences across the inner wall of Schlemm's canal, endothelial cells partially detach into transient, balloon-like structures termed "giant vacuoles." As pressure increases, the size and number of vacuoles increase in normal eyes.[18] Within these vacuoles are widely spaced pores through which aqueous humor enters the lumen of Schlemm's canal.[19] In glaucoma, there is a decrease in the number of pores.[20]

Though it was once believed that aqueous humor outflow was relatively uniform around the circumference of the anterior chamber, an important finding in glaucoma research over the last 10 years has been the recognition of regional differences in outflow. When the anterior chamber of enucleated human eyes has been perfused with fluorescent microbeads, areas experiencing a great deal of flow and collecting a large number of beads in the meshwork can be seen, as well as regions receiving almost no beads and carrying relatively little flow.[22] As IOP increases, areas of good flow become more and more restricted, partly due to collapse of Schlemm's canal.[23]

Alex Huang, MD, a glaucoma specialist and researcher at Ronald Reagan UCLA Medical Center, is using this information to pinpoint the best location to place a stent to improve aqueous humor outflow.[24] Intraoperatively, when fluorescein is perfused into the aqueous humor, its pathway can be mapped leaving the eye. Intraoperative images from Dr. Huang's work show the remarkable non-uniformity of outflow and ways in which high-flow regions can unexpectedly turn into low-flow areas, and vice versa.[24] The trigger for those shifts in flow is unknown at this time.

HOW MIOTICS REDUCE IOP

A traditional understanding of how miotics work to reduce IOP was that miotic-induced contraction of the longitudinal bundle of the ciliary muscle pulled the scleral spur down and backward. This resulted in "opening up" the meshwork, yielding improved aqueous outflow (i.e., decreased resistance) and a decrease in IOP. But given that the corneoscleral portion of the meshwork is attached to the scleral spur and makes essentially no contribution to normal outflow resistance, this raises the question of how opening up this portion of the meshwork, which already has essentially no resistance, could improve outflow.[17]

A closer review of the anatomy of the longitudinal portion of the ciliary muscle has recently given us a more probable mechanism for how miotics actually work to reduce IOP in glaucoma.

A careful review of ciliary muscle anatomy shows that most of the muscle fibers of the longitudinal bundle actually bypass the scleral spur, sending their tendons to make direct connections into the meshwork, even the inner wall of Schlemm's canal. This system of tendons is known as the "cribriform plexus."[21] As IOP increases, one known effect is to compress Schlemm's canal, leading to its partial collapse, which adds to outflow resistance. By contracting the ciliary muscle, however, the tendons of the longitudinal bundle resist this compression and potential collapse of Schlemm's canal by pulling on the inner wall of the canal. By doing so, outflow is sustained and improved, and IOP decreases. This new view of the role of the ciliary muscle in outflow does not preclude the possibility of a benefit from pulling the scleral spur down and back, but the principal clinical benefit of using miotics appears to be their effect on keeping Schlemm's canal open.

THE DISTAL PORTION

Collector Channels. Emerging from the outer wall of Schlemm's canal are approximately 30 vessels, known as "collector channels," which are not uniformly distributed around the eye. As collector channels move toward the surface of the sclera, each divides into several parallel channels. The earliest of these branches is the deep scleral plexus. This group of vessels branches further, to become the intrascleral venous plexus, before winding through the remainder of scleral thickness to join the episcleral veins.

Branching a vessel into parallel channels decreases total resistance to flow, so by continuously branching as the vessels move toward the surface of the sclera, they ensure the continued downhill pressure gradient to the episcleral blood vessels required for the passive outflow of aqueous humor.

SITE OF RESISTANCE

We know the uveal meshwork and the corneoscleral meshwork likely don't make measurable contributions to aqueous outflow resistance in the normal eye.[17] Similarly, the connective tissue matrix within the JCT region can't account for a significant portion of outflow resistance, and the inner wall and its pores cannot account for more than 10% of normal outflow resistance on their own.[25,26] Furthermore, the dimensions of unobstructed collector channels in the distal portions of the outflow pathway, beyond Schlemm's canal, appear to be too large to present any significant resistance to outflow.

Nonetheless, we know that this system must generate a resistance in order to create the back pressure that is IOP. New findings have helped pinpoint the site of resistance at least within the proximal part of the outflow pathway. When pressure-sensitive probes have been pushed from the lumen of Schlemm's canal, through the inner wall, toward the anterior chamber to identify the point at which a pressure drop was measured along this pathway, 75% of the pressure drop was within 14 microns of the inner wall.[27] This corresponds to the JCT region. From this study and others, we can deduce that the major site of regulated outflow resistance in the proximal portion of the conventional outflow pathway of the normal eye resides within the matrix of the JCT region, in concert with the basement membrane and inner wall of Schlemm's canal.

However, since none of the tissue elements in this region are capable of generating the known resistance to flow, a more complex dynamic must be at play. This phenomenon is called the "funneling effect."[28] Discovery of the funneling effect is one of the greatest leaps forward in our understanding of outflow in decades. The key to unraveling how resistance is created was the realization that the pores in the inner wall tend to be "widely" spaced, approximately 20 to 30 μm apart. Because of this wide spacing, pores constrain aqueous flow to limited preferential pathways through the JCT and inner wall, forcing flow through the JCT matrix to converge upon each pore as though it was the tip of a funnel. Modeling conventional outflow in this way and using known flow parameters for the normal human eye, a 30-fold increase in JCT resistance was predicted from this funneling effect.[28]

Areas of high flow in the meshwork show an open and more distended JCT region, whereas areas of low-flow exhibit a more compact JCT region.[29,30] Separation between the inner wall and JCT, which occurs in response to pressure elevation, appears to break the funneling effect. This opens more of the inner wall of Schlemm's canal to flow, and by creating additional parallel pathways, resistance is decreased and pressure falls.

If we accept that the regulated component of outflow in the proximal portion of the conventional outflow pathway can be explained by the funneling effect, it is important to recall the early work of the late Morton Grant, who showed that complete incision of the

THE MECHANISM OF ACTION OF RHO-KINASE INHIBITORS

Rho-kinase inhibits the dismantling of the cellular cytoskeleton, keeping cells properly tensioned to maintain their shape and responsiveness to stress and strain. Rho-kinase inhibitors interfere with maintenance of the cytoskeleton, making cells more floppy and creating a more pliable tissue.[31] Experimental studies reveal that application of rho-kinase inhibitors loosens the cytoskeletal architecture of the JCT region and its connections to the inner wall.[32-37] This causes the JCT region to distend, breaking the funneling effect.

meshwork into Schlemm's canal eliminated only 75% of the total resistance to outflow.[38] The rest must be resistance created in the distal portion of the outflow pathway in series with that in the proximal portion of the pathway. One source for this additional resistance was discovered using perfusion studies of bovine eyes and later confirmed to occur in human eyes.[39,40]

As pressure is increased in normal eyes, Schlemm's canal begins to collapse.[23] What has not been understood is that part of this response is due to focal herniation of the inner wall and the JCT region into the openings of the collector channels, creating partial or complete occlusion.[39] Experimental studies have shown that in normal eyes, if IOP is reduced, these sliding hernias come back out. However, in age-matched normal and glaucomatous eyes, researchers have found that in both sets of eyes, some of these collector channels will be permanently blocked such that the herniations don't slide back out.[41] Importantly, the number of permanently obstructed collector channels is much greater in glaucomatous than in normal eyes.[41]

We don't yet know whether this obstruction is a cause or effect of disease, but it is one of the first morphological findings in glaucomatous eyes that signals reduced aqueous outflow and increased resistance.

REGULATION OF CONVENTIONAL OUTFLOW

The Proximal Portion. We are finally beginning to unravel how the trabecular meshwork and inner wall sense and respond to pressure changes, and lead to compensatory activity of the cells to reestablish homeostasis.

Normal cells do not respond to an increase in pressure applied uniformly around their surface, because water (i.e., cytoplasm) is incompressible. What they can sense is stretch and strain when the tissue they are part of (e.g., trabecular meshwork sheets or lamina cribrosa) is forced to flex due to a pressure difference across that tissue. When normal cells in the JCT region sense tissue stretch or strain as a result of increased pressure, they release signaling molecules to upregulate a set of enzymes that are released in order to degrade extracellular matrix and reduce flow resistance. This family of proteases are the matrix metalloproteinases (MMPs).[42] At the same time, a set of matricellular proteins are activated to alter intracellular cytoskeletal rigidity and extracellular matrix tension.[43] As MMPs and matricellular proteins increase, the matrix breaks down and cells loosen, and aqueous humor exits more efficiently. To prevent IOP from dropping too far, the system also makes a series of inhibitors of MMPs known as tissue inhibitors of metalloproteinases (TIMPs) that curtail the degradation produced by MMPs. By augmenting MMPs and matricellular proteins, or TIMPs, stress and strain on cells caused by changes in flow/resistance, either up or down, are reduced. In the normal eye, this molecular process and others will continually regulate outflow resistance, keeping IOP within its normal range.

The Distal Portion. In Schlemm's canal, endothelial cells respond to shear stress. As pressure goes up and the lumen narrows, flow in the canal is compressed through narrower openings and shears against the endothelial cell lining. Shear stress is increased in the circumferential flow toward the closest collector channel.[44,45] There is a point at which IOP becomes so elevated that the shear begins to force pulsatile waves of flow within Schlemm's canal, which are unrelated to the vascular pulse.[44]

In normal flow regulation, shear stress can be relieved by triggering endothelial cells to produce nitric oxide synthase 3 (eNOS) and generate the vasodilator nitric oxide to dilate Schlemm's canal and decrease the shear.[45] Since NO also plays a role in reversing the effects of vasoconstriction, nitric oxide donors, especially those that are butylated, or butylated nitric oxide donor molecules (bunods), are being targeted at the optic nerve head for potential therapeutic effect.[46]

UVEOSCLERAL OUTFLOW PATHWAY

Whether aqueous leaves the eye via the conventional outflow pathway or the uveoscleral outflow pathway depends on whether flow carries it into the meshwork anterior or posterior to the scleral spur. Aqueous entering anterior to the spur passes into the conventional outflow pathway, and that passing posterior to the spur enters the uveoscleral pathway.

In the uveoscleral outflow pathway, fluid flows along the connective fascicles that interweave among the smooth muscle cells of the longitudinal bundle until it reaches the supraciliary space. It continues along the inner surface of the sclera toward the posterior segment and eventually leaves the eye through the sclera

or the emissarial canals used by the vortex veins (i.e., uveovortex outflow).[47] Current estimates suggest that uveoscleral outflow accounts for up to 45% of the total outflow in normal eyes, which decreases with age and in POAG.[47]

One way to lower elevated IOP in the unconventional pathway is to impact the process of tissue remodeling in the extracellular matrix. As previously mentioned, normal connective tissue turns over and is broken down by enzymes called matrix metalloproteinases (MMPs), after which new matrices are built with inhibitors of metalloproteinases (TIMPs). These processes are in a constant push-pull with each other to maintain an equivalent amount of matrix while replenishing it at the same time.

Prostaglandins are arachidonic acid metabolites that appear to interrupt the tissue remodeling of MMPs and TIMPs by favoring dissolution of the connective tissue matrix in the ciliary muscle. As the connective tissue matrix that interweaves between the bundles of muscle cells in the ciliary muscle becomes less dense, it becomes more permeable, triggering uveoscleral outflow to increase and IOP to decrease.[48] At present, this appears to be the primary mechanism of action of the clinically useful prostaglandins built around the originally discovered prostaglandin F2 alpha-1-isopropyl ester.[49]

Dr. Freddo is a Senior Fulbright Fellow and part-time professor of optometry at the MCP Health Sciences University in Worcester, Mass. Dr. Freddo served for 25 years as professor of ophthalmology, pathology, and anatomy at Boston University School of Medicine, and then professor and director of the School of Optometry and Vision Science at The University of Waterloo, before retiring in 2016. He is the recipient of the 2020 Optometric Glaucoma Society Research Excellence Award.

1. Riley MV. The chemistry of aqueous humor. In: Anderson RE, ed. Biochemistry of the Eye. Place of publication not identified: Amer. Academy of Ophthalmology; 1983.
2. Toris C. Lesser known aqueous outflow pathways. In: Proc. XVII Intl Congress of Eye Res. Buenos Aires, Argentina; 2006.
3. Freddo TF, Bartels SP, Barsotti MF, et al. The source of proteins in the aqueous humor of the normal rabbit. Invest Ophthalmol Vis Sci. 1990;31(1):125-37.
4. Barsotti MF, Bartels SP, Freddo TF, et al. The source of protein in the aqueous humor of the normal monkey eye. Invest Ophthalmol Vis Sci. 1992;33(3):581-95.
5. Bert RJ, Caruthers SD, Jara H, et al. Demonstration of an anterior diffusional pathway for solutes in the normal human eye with high spatial resolution contrast-enhanced dynamic MR imaging. Invest Ophthalmol Vis Sci. 2006;47(12):5153-62.
6. Freddo TF, Neville N, Gong H. Pilocarpine-induced flare is physiological rather than pathological, Experimental Eye Research. 2013;107: 37-43,.
7. McCannel CA, Heinrich SR, Brubaker RF. Acetazolamide but not timolol lowers aqueous humor flow in sleeping humans. Graefe's Arch Clin Exp Ophthalmol. 1992;230:518-20.
8. Morrison JC, Van Buskirk EM. Ciliary process microvasculature of the primate eye. Am J Ophthalmol. 1984;97(3):372-83.
9. Raviola G, Raviola E. Intercellular junctions in the ciliary epithelium. Invest Ophthalmol Vis Sci. 1978;17(10):958-81.
10. Freddo TF. Intercellular junctions of the ciliary epithelium in anterior uveitis. Invest Ophthalmol Vis Sci. 1987; 28(2):320-9.
11. Larsson LI, Rettig ES, Brubaker RF. Aqueous flow in open-angle glaucoma. Arch Ophthalmol. 1995 Mar;113(3):283-6.
12. Nau CB, Malihi M, McLaren JW, et al. Circadian variation of aqueous humor dynamics in older healthy adults. Invest Ophthalmol Vis Sci. 2013 Nov; 54(12): 7623-29.
13. McCannel CA, Heinrich SR, Brubaker RF. Acetazolamide but not timolol lowers aqueous humor flow in sleeping humans. Graefe's Arch Clin Exp Ophthalmol. 1992;230:518-20.
14. Sit, AJ and McLaren J. Measurement of episcleral venous pressure. Experimental Eye Research 2011 93:291-8.
15. Greenfield DS. Glaucoma associated with elevated episcleral venous pressure. J Glaucoma. 2000 9:190-194.
16. Freddo, T. Anatomy of the Aqueous Outflow Pathways. In: Anatomy of the Eye and the Orbit: The Clinical Essentials. Cptr 9. Freddo T and Chaum E. Wolters and Kluwer. 2016.
17. Freddo T, Johnson M. Aqueous humor dynamics I; Measurement methods and animal studies. In Civan M, Benos D, Simon S (Eds.) The Eye's Aqueous Humor. Cambridge, MA: Academic Press. 2008.
18. Tripathi RC. Aqueous outflow pathway in normal and glaucomatous eyes. Br J Ophthalmol. 1972 56:157-74.
19. Johnson M, Shapiro A, Ethier CR, et al. Modulation of outflow resistance by the pores of the inner wall endothelium. Invest Ophthalmol Vis Sci. 199233(5):1670-5.
20. Johnson M, Chan D, Read AT, et al. The pore density in the inner wall endothelium of Schlemm's canal of glaucomatous eyes. Invest Ophthalmol Vis Sci. 2002 43:2950-5.
21. Rohen JW, Futa R, Lütjen-Drecoll E. The fine structure of the cribriform meshwork in normal and glaucomatous eyes as seen in tangential sections. Invest Ophthalmol Vis Sci. 1981 Oct;21(4):574-85.
22. Cha DK, Cha JX, Gong L, et al. Variations in active outflow along the trabecular outflow pathway. Exp Eye Res. 2016;146:354-60.
23. Johnson MC, Kamm RD. The role of Schlemm's canal in aqueous outflow from the human eye. Invest Ophthalmol Vis Sci. 1983 Mar;24(3):320-5.
24. Huang AS, Penteado RC, Papoyan V, et al. Aqueous angiographic outflow improvement after trabecular microbypass in glaucoma patients. Ophthalmol Glaucoma. 2019 Jan-Feb;2(1):11-21.
25. Bill A, Svedbergh B. Scanning electron microscopic studies of the trabecular meshwork and the canal of Schlemm--an attempt to localize the main resistance to outflow of aqueous humor in man. Acta Ophthalmol (Copenh). 1972 50:295-320.
26. Moseley H, Grierson I, Lee WR. Mathematical modeling of aqueous humour outflow from the eye through the pores in the lining endothelium of Schlemm's canal. Clin Phys Physiol Meas Off J Hosp Phys Assoc Dtsch Ges Med Phys Eur Fed Organ Med Phys. 1983;4:47-63.
27. Maepea O and Bill A. Pressures in the juxtacanalicular tissue and Schlemm's canal in monkeys. Exp Eye Res. 1992;54:879-83.
28. Johnson M, Shapiro A, Ethier CR, et al. Modulation of outflow resistance by the pores of the inner wall endothelium. Invest Ophthalmol Vis Sci. 1992 33:1670-75.
29. Yang C-YC, Liu Y, Lu Z, et al. Effects of Y27632 on aqueous humor outflow facility with changes in hydrodynamic pattern and morphology in human eyes. Invest Ophthalmol Vis Sci. 2013;54:5859-70.
30. Cha EDK, Xu J, Gong L, et al. Variations in active outflow along the trabecular outflow pathway. Exp Eye Res. 2016 146:354-60.
31. Lu Z, Overby DR, Scott PA, et al. The mechanism of increasing outflow facility by rho-kinase inhibition with Y-27632 in bovine eyes. Exp Eye Res. 2008 86:271-81.
32. Ren R, Li G, Le TD, et al. Netarsudil increases outflow facility in human eyes through multiple mechanisms. Invest Ophthalmol Vis Sci. 2016 57:6197-209.
33. Lu Z, Zhang Y, Freddo TF, et al. Similar hydrodynamic and morphological changes in the aqueous humor outflow pathway after washout and Y27632 treatment in monkey eyes. Exp Eye Res. 2011 93:397-404.
34. Yang C-YC, Liu Y, Lu Z, et al. Effects of Y27632 on aqueous humor outflow facility with changes in hydrodynamic pattern and morphology in human eyes. Invest Ophthalmol Vis Sci. 2013 54:5859-70.
35. Sabanay I, Gabelt BT, Tian B, et al. H-7 effects on the structure and fluid conductance of monkey trabecular meshwork. Arch Ophthalmol Chic Ill 2000 118:955-62.
36. Sabanay I, Tian B, Gabelt BT, et al. Functional and structural reversibility of H-7 effects on the conventional aqueous outflow pathway in monkeys. Exp Eye Res. 2004 78:137-50.

37. Lai J, Su Y, Swain DL, et al. The role of Schlemm's canal endothelium cellular connectivity in giant vacuole formation: A 3-D electron microscopy study. Invest Ophthalmol Vis Sci. 2019 60(5):1630-43.
38. Grant WM. Experimental aqueous perfusion in enucleated human eyes. Arch Ophthalmol. 1963 69:783-801.
39. Battista SA, Lu Z, Hofmann S, et al. Reduction of the available area for aqueous humor outflow and increase in meshwork herniations into collector channels following acute IOP elevation in bovine eyes. Invest Ophthalmol Vis Sci. 2008 49:5346-52.
40. Hann CR, Vercnocke AJ, Bentley MD, et al. Anatomic changes in Schlemm's canal and collector channels in normal and primary open-angle glaucoma eyes using low and high perfusion pressures. Invest Ophthalmol Vis Sci. 2014 19;55:5834-41..
41. Gong H. The histopathological changes in the trabecular outflow pathway and their possible effects on aqueous outflow in eyes with primary open-angle glaucoma. In: Knepper PA, Samples JR, eds. Glaucoma Research and Clinical Advances 2016 to 2018. Amsterdam, the Netherlands: Kugler Publishers. 17-40, 2016.
42. Alexander JP, Samples JR, Van Buskirk EM et al. Expression of matrix metalloproteinases and inhibitor by human trabecular meshwork. Invest Ophthalmol Vis Sci. 1991;32:172-80.
43. Rhee DJ, Haddadin RI, Kang MH, et al. Matricellular proteins in the trabecular meshwork. Exp Eye Res. 2009;88:694-703.
44. Sherwood JM, Stamer WD, Overby DR. A model of the oscillatory mechanical forces in the conventional outflow pathway. J. R. Soc. Interface2019 16: 20180652.
45. Ashpole, NE, Overvy DR, Ethier CR, et al. Shear stress-triggered nitric oxide release from Schlemm's canal cells. Invest Ophthalmol Vis Sci. 2013;55:8067-76.
46. Sugiyama T, Oku H, Kojima S, et al. Effect of a nitric oxide donor on optic nerve head circulation. [Article in Japanese] Nippon Ganka Gakkai Zasshi. 1996;100:5-10.
47. Alm A, Nilsson S. Uveoscleral outflow-a review. Exp Eye Res. 2009 88:760-8.
48. Lutjen-Drecoll E, Tamm E. Morphological study of the anterior segment of cynomolgus monkey eyes following treatment with prostaglandin F2 alpha. Exp Eye Res 1988;47:761-9.
49. Camras CB, Siebold EC, Lustgarten JS, et al. Maintained reduction of intraocular pressure by prostaglandin F2 alpha-1-isopropyl ester applied in multiple doses in ocular hypertensive and glaucoma patients. Ophthalmology. 1989;96:1329-37.

OPTIC NERVE ASSESSMENT

Examining the Optic Nerve

Peter Lalle, OD, FAAO

In my 35-plus years training optometric students and residents at the Baltimore VA Medical Center, I worked with very bright students from every optometry school around the country. They were energetic, promising young optometrists, but they suffered from one major shortcoming: They had difficulty evaluating the optic nerve. I came to realize that this was not unique to my facility, but was a universal problem. As such, I investigated why our future optometrists had difficulty evaluating this critical piece of anatomy that played a pivotal role in glaucoma diagnosis.

First, I asked my residents how they were taught about glaucoma. Not surprisingly, everyone had a different answer. I asked more specifically: *How were you taught about the optic nerve? What were the essential skills you had to know about evaluating the optic nerve? Did your professors show you stereo slides? Did you have one-on-one mentoring to improve your optic nerve assessment?* That's usually when my residents grew silent. They couldn't describe exactly how they were taught. Moreover, few were shown stereo photos, and almost none had used textbooks that might have offered additional insights.

I was trained in the 1970s with a direct ophthalmoscope, but I realized that little has changed since then. So I considered whether there was a better way to teach the optic nerve evaluation in today's digital world.

A PERSONAL QUEST TO IMPROVE OPTIC NERVE EXAMINATION

For about two decades, we used a Nidek 3Dx camera that took simultaneous stereoscopic photographs, meaning the parallax was fixed. It was an easy camera to use and offered magnified stereo slides of the optic nerve. When I mentored students and residents in the clinic, we used an inexpensive, handheld 3D slide viewer to view the images. We would take time to go over the optic nerve assessment, and I would highlight certain features. I would hold up an image and ask, "Tell me what you see." Typically, the residents would immediately zero in on the cup-to-disc (C/D) ratio, so I would stop them and say, "Let's start at the retina. Tell me what the retina looks like." They would describe the retina and jump back to the optic nerve again. "No," I would say. "Let's first talk about peripapillary atrophy, is it there or not?" Then we would move to the disc margins and whether Elschnig's ring—the outer boundary of the rim tissue—was visible, and further discuss the rim, using vessel bend as a benchmark. Down the road, I used digital images instead of slides, and as each resident finished, I added arrows to the digital images to point out specific features. I was trying to teach these inexperienced clinicians a systematic approach to examining the optic nerve.

The optic nerve displayed in Figure 1 is an example of a slide I use in a workshop I developed to improve optic nerve evaluation. In the image, which can't properly be assessed unless it is seen in stereo, the key features are an exceptionally wide and prominent scleral ring, a very small disc, and a larger color

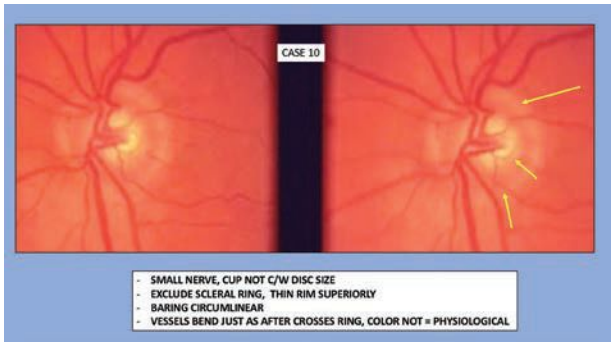

FIGURE 1. OPTIC NERVE SLIDE IN WORKSHOP.
This optic nerve image is an example of a slide used in my workshop. *Images: Peter Lalle, OD, FAAO*

cup than would be expected for such a small disc. In addition, the baring of a circumlinear vessel can be seen inferotemporally—an early sign of optic nerve damage. Furthermore, one of the small vessels, an arterial or venule, dives down as soon as it crosses the scleral ring. While the rim of the color cup looks much wider in this area, the rim of the physiologic cup bends almost immediately. This is a very thin rim superiorly with practically no rim inferiorly—indicating this patient is at high risk for glaucoma.

IS OPHTHALMOSCOPY STILL RELEVANT IN AN OCT WORLD?

One question is whether ophthalmoscopy is still relevant today given the prevalence of optical coherence tomography (OCT). While OCT has many benefits for tracking structural damage in established and at-risk glaucoma patients, a limiting aspect to the technology is its widely reported artifacts, as demonstrated by some of the following findings in the literature.

One group of researchers assessing 131 macular thickness and 277 nerve fiber layer (NFL) scans from spectral-domain OCT found that 28% and 20% of the images, respectively, had artifacts.[1] Other investigators looking at OCT imaging of the NFL found that 46.3% of 2,313 eye scans had at least one artifact.[2]

In addition to artifacts, OCT is known to have floor and ceiling effects. For example, in one case, a legally blind left eye appeared to have a thicker NFL than the sighted right eye. An error in the segmentation algorithm incorrectly measured the thickness of the underlying layers in the absence of NFL, creating a floor effect. In addition, the OCT erroneously calculated the vertical C/D ratio as 0.9 for an NLP eye, so there seemed to be a limit to how large the C/D ratio could be measured—a kind of optic nerve analysis cap.

A recent study from Öhnell HM, et al. compared circumpapillary RNFL (cpRNFL) scans from 69 healthy individuals and 49 glaucoma patients to those taken 10 years earlier, to evaluate the performance of OCT progression analyses.[3] Paradoxically, the OCT reported the average cpRNFL appeared to have thickened in those eyes with advanced glaucoma (MD≥-10dB). This was due to the floor effect, as noted above. Further, for 30% of healthy individuals, one of three OCT progression analyses incorrectly indicated progression, and the analyses as a whole generated a relatively high percentage of false positives. In addition, 27% of cases had to be excluded from analysis because the OCT couldn't produce sufficient-enough quality scans or re-scans. So, another issue with the OCT is that the software doesn't always obtain meaningful data. Often times, the technology dutifully reports metrics that are focused in the wrong direction.

Furthermore, OCT analyses are interpreted relative to normal ranges, and such databases allow for a wide range of accepted limits for normal. The patient has to lose quite a bit of NFL before being classified as having glaucomatous damage. For example, according to the normal range of RNFL thickness values established by a group of researchers in 2005[4], a 69-year-old at the 95th percentile with an RNFL of 107µm could lose 30% of RNFL thickness and still be considered normal. More than 30 years ago, Harry Quigley, MD, found that an individual had lose 25 to 40% of their axons before an NFL defect was apparent on VFs,[5,6] for perspective on where we are at today.

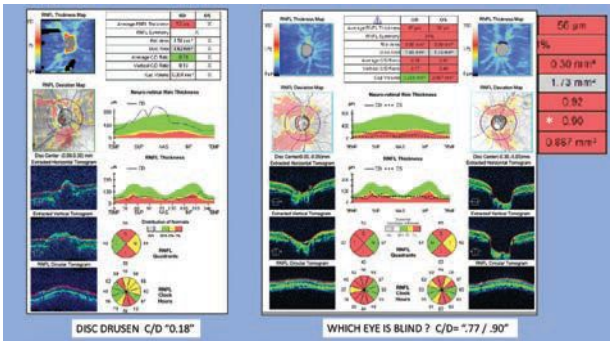

FIGURE 2. FLOOR AND CEILING EFFECT.
The OCT incorrectly reported the cup and vertical C/D ratio, due to a floor and ceiling effect.

Although most glaucoma clinicians have switched from direct to indirect ophthalmoscopy, one major problem persisting with this ubiquitous technology is evaluating the resulting images is subjective and nuanced. As a result, inter- and intraobserver discrepancies and errors can confound findings.

One classic study from Paul Lichter, MD, found poor interobserver agreement among glaucoma experts asked to evaluate monocular and stereo slides.[7] Thirty years later, researchers compared then state-of-the-art devices to experts grading stereo photos, and the experts had the largest area underneath the curve.[8] A similar study in 2009 by Vessani, et al., added general ophthalmologists to the subject pool and found that the technology was better at grading than general ophthalmologists, but glaucoma experts still beat the devices.[9] Another paper showed that discordance was frequent and substantial among five glaucoma specialists' optic disc margin, rim margin, and rim width estimates.[10]

Factors that reportedly impact the level of discordance between clinicians in evaluating the optic disc for glaucoma are level of training, expertise, and overall experience.

In 2011, a team evaluated glaucoma specialists' and general ophthalmologists' ability to identify disc and rim margins, and certain areas of the optic nerve, using serial stereo photos, and found interobserver agreement of general ophthalmologists was

significantly lower than that of specialists, which was moderate.[11] However, after the non-experts received a training session, interobserver agreement and accuracy showed a small, but statistically significant, improvement.

One study[12] led by Lisa Abrams, MD, reported that ophthalmologists had higher interobserver agreement in estimating C/D ratio and were more sensitive in assessing glaucomatous optic nerve damage than optometrists. In response, John Spalding, OD, authored a study[13] in which he assembled a larger group of optometrists, some of whom had worked with glaucoma patients. He investigated agreement among optometrists in assessing C/D ratios and glaucomatous damage, and analyzed the results according to residency training, practice setting, and glaucoma patient experience, and showed that training, whether by residency or experience, made a difference in observations.

From these studies, it became clear to me that a standard criterion for evaluating and teaching the optic nerve would be helpful.

EFFORTS TO IMPROVE CLINICAL EVALUATION OF THE OPTIC NERVE

For a number of years, clinicians have been using various lenses and techniques to measure the size of the disc and cup in an attempt to reduce inter- and intraobserver error and get an accurate size of the disc.

In 2002, George Spaeth, MD, published his Disc Damage Likelihood Scale (DDLS) based on the appearance of the optic disc's neuroretinal rim, corrected for disc diameter.[14] Dr. Spaeth put forth that a thin rim and a large disc was acceptable, but a thin rim and a small disc was not.

Since then, a number of programs have become available to help trainers, trainees, and clinicians improve their evaluation skills. For example, the Iowa Glaucoma Curriculum from Wallace L.M. Alward, MD, is an online textbook on glaucoma that offers insights to improve optic nerve evaluation.

In addition, Belgian ophthalmologist Thierry Zeyen, MD, PhD, built a website to teach optic nerve head evaluation. The online training site shows practitioners baseline and follow-up stereo photos to evaluate and then decide if the optic nerve has progressed. The cases feature advanced disease, and since OCT is reportedly less adept at visualizing advanced disease overall,[15] direct observation of the optic nerve is an important skill to reinforce.

Murray Fingeret, OD, published a paper on the five rules to assess the optic disc known as the "5 Rs" to evaluate the optic disc and retinal nerve fiber layer for glaucoma.[16] The rules included: identify the scleral ring, identify the size of the neuroretinal rim, examine the RNFL, examine the parapapillary atrophy region, and watch for retinal or optic disc hemorrhages. Of note, the authors emphasized rim and disc size rather than C/D ratio.

The GONE (Glaucomatous Optic Neuropathy Evaluation) project is an online initiative developed in 2008 at the Centre for Eye Research Australia and Royal Victorian Eye and Ear Hospital, to help teaching and evaluation of optic disc assessment.[17] The free program has seen more than 20,000 people go through it, and ophthalmologists from around the world have joined the initiative.

FIGURE 3. GONE (GLAUCOMATOUS OPTIC NEUROPATHY EVALUATION) PROJECT
The GONE (Glaucomatous Optic Neuropathy Evaluation) Project is an online initiative to help teaching and evaluation of optic disc assessment.

In the GONE program, the viewer is shown a (non-stereo) photo, and given 90 seconds to analyze nine features of the optic nerve and then decide if glaucoma is present. Post-evaluation, the program shows how the answers compare to past responses and ranks the attendee's percentile. One study derived from GONE[18] assessed the ability of glaucoma subspecialists, general ophthalmologists, and trainees to evaluate 42 monoscopic optic disc photos of healthy and glaucomatous eyes, using the subspecialists as the gold standard. It found the general ophthalmologists and trainees underestimated glaucoma by 22% and 23%, respectively, and overestimated it by 8.9% and 13%, respectively, often in cases of larger optic discs.

In 1997, a group of British ophthalmologists published a paper[19] about a very accurate and reproducible method of determining the size of the disc and C/D ratio. The researchers built a ring to hold a graticule and attached it to a 60-diopter lens to measure the vertical diameters of the cup disc and arrive at the C/D ratio. In 29 eyes, the researchers found good agreement between measurements, and exceptional agreement with the C/D ratio—such that if a change occurred in the C/D ratio assessment of >0.1, the likelihood that it was false-positive was <5%.

Finally, the American Academy of Ophthalmology (AAO) in its Basic and Clinical Science Course recommends 11 key features of an optic nerve be evaluated in every case. They include large C/D ratio, asymmetry of cups (taking disc size into consideration), generalized enlargement, focal enlargement, drance hemorrhages (disc hemorrhages within the peripapillary RNFL layer), vessel overpass, NFL loss, peripapillary atrophy in the beta zone, rim translucency, vessel nasalization, and baring of the circumlinear vessel. The AAO notes that C/D ratio alone is not an adequate assessment and that disc size must be considered.

NEED FOR ADDITIONAL TRAINING

The information uncovered during my search to improve optic nerve evaluation reinforced that additional training would be beneficial to many optometry students. I believe we can positively impact our future clinicians' ability to evaluate the optic nerve. Once students can incorporate the features learned into their assessment, they're better able to look for them and more accurately discern the true risk for glaucoma.

An interventional study is underway to determine if the workshop I have developed can prove to be a beneficial tool to improve optic nerve evaluation. Both a pre- and post-test are administered to participants, and are compared, to determine the workshop's effectiveness. The workshop can be held virtually via Zoom. In addition to students and residents, this workshop can be administered to any group interested in improving evaluation of the glaucomatous optic nerve. A sample of the workshop is available for viewing on vimeo or YouTube here:
https://vimeo.com/373647096
https://www.youtube.com/watch?v=DUBaG929QrU&t=4s

Dr. Lalle served as the chief of optometry at Baltimore VA Medical Center from 1981 to 2016, and is a founding member of the Optometric Glaucoma Society.

1. Asrani S, Essaid L, Alder BD, et al. Artifacts in spectral-domain optical coherence tomography measurements in glaucoma. JAMA Ophthalmol. 2014;Apr1;132(4):396-402.
2. Liu Y, Simavli H, Que CJ, et al. Patient characteristics associated with artifacts in Spectralis optical coherence tomography imaging of the retinal nerve fiber layer in glaucoma. Am J Ophthalmol. 2015 Mar;159(3):565-76.e2.
3. Öhnell HM, Heijl A, Bengtsson B. Ageing and glaucoma progression of the retinal nerve fibre layer using spectral domain optical coherence tomography analysis. Acta Ophthalmologica. 2020; Aug. 9. [Epub ahead of print].
4. Budenz DL, Michael A, Chang RT, et al. Sensitivity and specificity of the StratusOCT for perimetric glaucoma. Ophthalmology. 2005 Jan;112(1):3-9.
5. Quigley HA, Dunkelberger GR, Green WR. Retinal ganglion cell atrophy correlated with automated perimetry in human eyes with glaucoma. Am J Ophthalmol. 1989;107:453-64.
6. Kerrigan-Baumrind LA, Quigley HA, PeaseME, et al. Number of ganglion cells in glaucoma eyes compared with threshold visual field tests in the same persons. Invest Ophthalmol Vis Sci. 2000;41:741-8.
7. Lichter PR. Variability of expert observers in evaluating the optic disc. Trans Am Ophthalmol Soc. 1976;74:532-72.
8. Deleón-Ortega JE, Arthur SN, McGwin G Jr, et al. Discrimination between glaucomatous and nonglaucomatous eyes using quantitative imaging devices and subjective optic nerve head assessment. Invest Ophthalmol Vis Sci. 2006 Aug;47(8):3374-80.
9. Vessani RM, Moritz R, Batis L, et al. Comparison of quantitative imaging devices and subjective optic nerve head assessment by general ophthalmologists to differentiate normal from glaucomatous eyes. J Glaucoma. 2009 Mar;18(3):253-61.
10. Hong SW, Koenigsman H, Ren R, et al. Glaucoma Specialist Optic Disc Margin, Rim Margin, and Rim Width Discordance in Glaucoma and Glaucoma Suspect Eyes. Am J Ophthalmol. 2018 Aug;192:65-76.
11. Breusegem C, Fieuws S, Stalmans I, et al. Agreement and accuracy of non-expert ophthalmologists in assessing glaucomatous changes in serial stereo optic disc photographs. Ophthalmology. 2011 Apr;118(4):742-6.
12. Abrams LS, Scott IU, Spaeth GL, et al. Agreement among optometrists, ophthalmologists, and residents in evaluating the optic disc for glaucoma. Ophthalmology. 1994 Oct;101(10):1662-7.
13. Spalding JM, Litwak AB, Shufelt CL. Optic nerve evaluation among optometrists. Optom Vis Sci. 2000 Sep;77(9):446-52.
14. Spaeth GL, Henderer J, Liu C, et al. The disc damage likelihood scale: reproducibility of a new method of estimating the amount of optic nerve damage caused by glaucoma. Trans Am Ophthalmol Soc. 2002;100:181-5; discussion 185-6.
15. Zhang X, Dastiridou A, Francis BA, et al. Advanced imaging for glaucoma study group. comparison of glaucoma progression detection by optical coherence tomography and visual field. Am J Ophthalmol. 2017 Dec;184:63-74.
16. Fingeret M, Medeiros FA, Susanna R Jr. et al. Five rules to evaluate the optic disc and retinal nerve fiber layer for glaucoma. Optometry. 2005 Nov;76(11):661-8.
17. Kong YX, Coote MA, O'Neill EC, et al. Glaucomatous optic neuropathy evaluation project: a standardized internet system for assessing skills in optic disc examination. Clin Exp Ophthalmol. 2011 May-Jun;39(4):308-17.
18. O'Neill EC, Gurria LU, Pandav SS, et al. Glaucomatous optic neuropathy evaluation project: factors associated with underestimation of glaucoma likelihood. JAMA Ophthalmol. 2014 May;132(5):560-6.
19. Haslett RS, Batterbury M, Cuypers M, et al. Inter-observer agreement in clinical optic disc measurement using a modified 60 D lens. Eye (Lond).1997;11(Pt 5):692-7.

ABOUT THE OPTOMETRIC GLAUCOMA SOCIETY AND THE OPTOMETRIC GLAUCOMA FOUNDATION

The Optometric Glaucoma Society's (OGS) mission is to promote excellence in the care of glaucoma patients through professional education and scientific investigation. The Optometric Glaucoma Foundation (OGF) is the educational foundation of the OGS whose mission is to support glaucoma education for the optometric profession. This includes supporting and developing educational programs for students, residents, educators and practitioners. The OGF will work with different groups to meet its goals including industry and educational institutions, as well as optometric and ophthalmologic organizations. For more information: www.optometricglaucomasociety.org

VYZULTA®

(latanoprostene bunod ophthalmic solution), 0.024%

Available in 2.5 and 5 mL bottles at pharmacies nationwide.

For more information, visit vyzultanow.com

BAUSCH+LOMB